

Chapter 15

BEAM BREAKUP

In a high-energy electron linac*, the relative longitudinal positions of the beam particles inside a bunch do not change. Thus, the tail particles are always affected by the head particles. We have shown that the longitudinal wake will cause the tail particles to lose energy. This loss, accumulated throughout the whole length of the linac, can be appreciable, leading to an undesirable spread in energy within the bunch. If the linac is the upstream part of a linear collider, this energy spread will have chromatic effect on the final focusing and eventually enlarging the spot size of the beam at the interaction point. We have also discussed how this energy spread can be corrected by placing the center of the bunch at an rf phase angle where the rf voltage gradient is equal and opposite to the energy gradient along the bunch.

Here, we would like to address the effect of the transverse wake potential. A small offset of the head particles will translate into a transverse force on the particles following. The deflections of the tail particles will accumulate along the linac. When the particles hit the vacuum chamber, they will be lost. Even if the aperture is large enough, the transverse emittance will be increased to an undesirable size. This phenomenon is called *beam breakup*. This is not a collective instability, however.

Recently, there is a lot of interest in isochronous or quasi-isochronous rings, where the spread in the slippage factor for all the particles in the bunch is very tiny, for example, $\Delta\eta \lesssim 10^{-6}$. In some of these rings, like the muon colliders where the beam is stored

*All proton linacs in existence are not ultra-relativistic. The highest energy is less than 1 GeV. Therefore synchrotron oscillations occur.

to about 1000 turns, the head and tail particles hardly exchange longitudinal position, and we are having a situation very similar to linacs. Problems of beam breakup will also show up in these rings. The beam breakup discussed in this chapter does not allow particles to exchange longitudinal positions or change their longitudinal positions. We therefore assume that their velocities are equal to the velocity of light.

15.1 Two-Particle Model

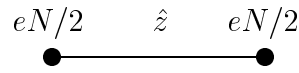


Figure 15.1: The two-particle model, where the bunch is represented by two macro-particles each carrying half the charge of the bunch separated by a distance \hat{z} .

Take the simple two-particle model in Fig. 15.1, by which the bunch is represented by two macro-particles of charge $\frac{1}{2}eN$ separated by a distance \hat{z} . The transverse displacements of the head, y_1 , and the tail, y_2 , satisfy

$$\frac{d^2 y_1}{ds^2} + k_{\beta_1}^2 y_1 = 0, \quad (15.1)$$

$$\frac{d^2 y_2}{ds^2} + k_{\beta_2}^2 y_2 = -\frac{e^2 N W_1(\hat{z})}{2L E_0} y_1, \quad (15.2)$$

where E_0 is the energy of the beam particles and s is the longitudinal distance measured along the designed particle path, W_1 is the transverse wake function for one linac cavity of length L , and k_β is the betatron wave number. For an isochronous ring, L will be taken as the ring circumference $C = 2\pi R$ and

$$k_\beta = \frac{\nu_\beta}{R} = \frac{1}{\langle \beta \rangle}, \quad (15.3)$$

where ν_β is the betatron tune and $\langle \beta \rangle$ is the average betatron function. We can also define a betatron tune $\nu_\beta = L k_\beta / (2\pi)$ for a linac as the number of betatron oscillations a particle makes along the whole length L of the linac. This model has been giving a reasonably accurate description to the beam breakup mechanism for short electron bunches when \hat{z} is taken as the rms bunch length. The head makes simple harmonic motion $y_1(s) = y_{10} \cos k_\beta s$ according to Eq. (15.1), where y_{10} is its initial displacement.

If the tail is initially at $y_2 = y_{10}$ with $y_2' = dy_2/ds = 0$, its displacement can be readily solved and the result is

$$y_2(s) = y_{10} \cos \bar{k}_\beta s \cos \frac{\Delta k_\beta s}{2} - y_{10} \sin \bar{k}_\beta s \left[\frac{\Delta k_\beta}{2} + \frac{e^2 N W_1(\hat{z})}{4 L E_0 \bar{k}_\beta} \right] \left[\frac{\sin \Delta k_\beta s / 2}{\Delta k_\beta / 2} \right], \quad (15.4)$$

where $\bar{k}_\beta = \frac{1}{2}(k_{\beta_1} + k_{\beta_2})$ is the mean of the two betatron wave numbers of the head and tail. When the tune difference $\Delta k_\beta = k_{\beta_2} - k_{\beta_1}$ approaches zero, the tail is driven resonantly by the head and its displacement grows linearly with s :

$$y_2(s) = y_1(s) - \frac{e^2 N W_1(\hat{z})}{4 E_0 L k_\beta} [y_{10} \sin k_{\beta_1} s] s. \quad (15.5)$$

In the length ℓ , the displacement of the tail will grow by Υ folds, where [2]

$$\Upsilon = -\frac{e^2 N W_1(\hat{z}) \ell}{4 E_0 L k_\beta} = -\frac{e^2 N W_1(\hat{z}) \langle \beta \rangle \ell}{4 E_0 L}, \quad (15.6)$$

and $W_1(\hat{z})$ is negative for small \hat{z} . In the above, we have written the growth in term of the average betatron function $\langle \beta \rangle$. This is because the transverse impedance initiates a kick y' of the beam and the size of the kicked displacement depends on the betatron function at the location of the impedance. This can be easily visualized from the transfer matrix.

For a broadband impedance, the transverse wake function at a distance z behind the source particle is, for $z > 0$,

$$W_1(z) = -\frac{\omega_r^2 Z_1^\perp}{Q \bar{\omega}} e^{-\alpha z / c} \sin \frac{\bar{\omega} z}{c}, \quad (15.7)$$

where Z_1^\perp is the transverse impedance at the angular resonant frequency ω_r , which is shifted to $\bar{\omega} = \sqrt{\omega_r^2 - \alpha^2}$ by the decay rate $\alpha = \omega_r / (2Q)$ of the wake with Q being the quality factor. Let us introduce the dimensionless variables

$$v = \frac{\omega_r \sigma_\ell}{c}, \quad t = \frac{z}{\sigma_\ell}, \quad \text{and} \quad \phi = vt \cos \phi_0 = \frac{\bar{\omega} z}{c}, \quad (15.8)$$

where the angle ϕ_0 is defined as

$$\cos \phi_0 = \sqrt{1 - \frac{1}{4Q^2}} \quad \text{or} \quad \sin \phi_0 = \frac{1}{2Q}, \quad (15.9)$$

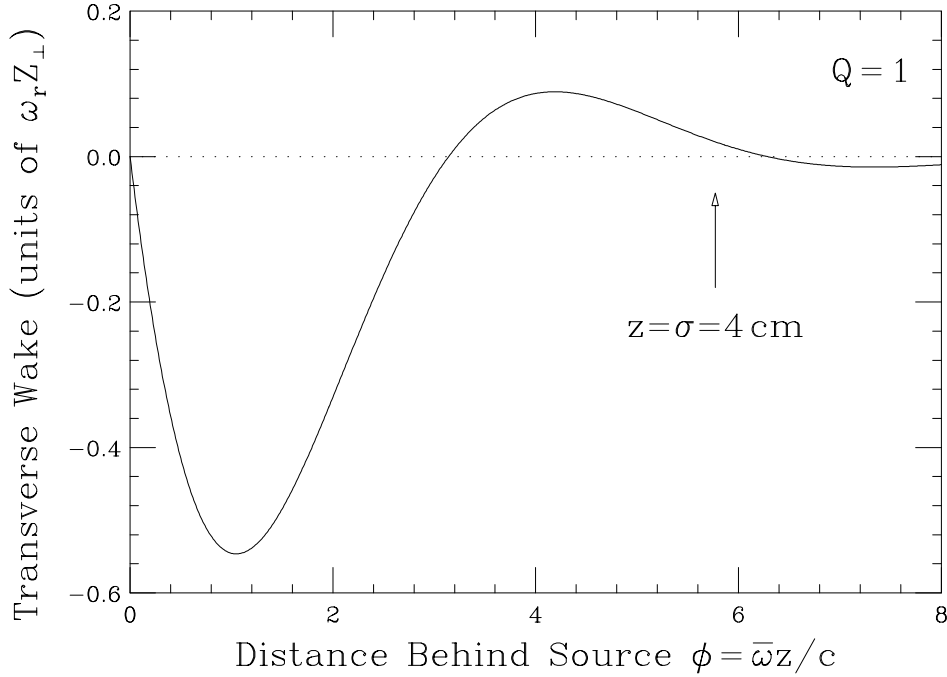


Figure 15.2: Transverse wake function for a broadband impedance with $Q = 1$ in units of $\omega_r Z_1^\perp$ as a function of $\phi = \bar{\omega}z/c$ behind the source. With resonant angular frequency $\omega_r = 50$ GHz, the position for $z = \sigma_\ell$ for the 4-cm bunch is marked, which is certainly outside the linear region and the 2-particle model will not apply.

assuming that $Q > \frac{1}{2}$. Then, the transverse wake in Eq. (15.7) can be rewritten as, for $\phi > 0$,

$$W_1(\phi) = -2\omega_r Z_1^\perp \tan \phi_0 \sin \phi e^{-\phi \tan \phi_0}, \quad (15.10)$$

The wake function decreases linearly from zero when $\phi = \bar{\omega}z/c \ll 1$ and reaches a minimum

$$W_1|_{\min} = -2\omega_r Z_1^\perp \tan \phi_0 \cos \phi_0 e^{-(\frac{\pi}{2} - \phi_0) \tan \phi_0} \quad (15.11)$$

at

$$\phi = \frac{\pi}{2} - \phi_0 \quad \text{or} \quad \frac{\alpha z}{c} = \left(\frac{\pi}{2} - \phi_0 \right) \tan \phi_0. \quad (15.12)$$

After that it oscillates with amplitude decaying at the rate of $\alpha = \omega_r/(2Q)$, crossing zero at steps of $\Delta\phi = \bar{\omega}z/c = \pi$. This is illustrated in Fig. 15.2.

Obviously, the growth expression of Eq. (15.6) does not apply to all bunch lengths. For example, if \hat{z} just happens to fall on the first zero of $W_1(\hat{z})$, Eq. (15.6) says there is

no growth at all. However, particles in between will be deflected and they will certainly affect the tail particle. Thus, the criterion for Eq. (15.6) to hold is the variation of the wake function along the bunch must be smooth. In other words, we must be in the linear region of the wake function, or

$$\phi = \frac{\bar{\omega}z}{c} \ll 1 \quad \longrightarrow \quad \sigma_\ell \ll \frac{1}{2} \frac{\lambda}{2\pi}, \quad (15.13)$$

i.e., the rms bunch length must be less than half the reduced wavelength λ of the resonant impedance. As an example, if the broadband impedance with $Q \sim 1$ has resonant frequency 7.96 GHz ($\omega_r = 50$ GHz), the two-particle model works only when the rms bunch length $\sigma_\ell \ll 3$ mm. Therefore, the model cannot be applied to the usual proton bunches. For the 50 GeV on 50 GeV muon collider, the muon bunches have an rms length of 4 cm, and will not be able to fit into this model also.

15.2 Long Bunch

For a bunch with linear density $\rho(z)$, the transverse motion $y(z, s)$ at a distance z behind the bunch center and at position s along the linac is given by

$$\frac{d^2 y(z, s)}{ds^2} + k_\beta^2 y(z, s) = -\frac{e^2 N}{LE_0} \int_{-\infty}^z dz' \rho(z') W_1(z - z') y(z', s). \quad (15.14)$$

This equation can be solved first by letting $y(z, s)$ be a free oscillation on the right-hand side and solving for the displacement $y(z, s)$ on the left-hand side. Then, iterations are made until the solution becomes stable. Therefore, when Υ is large, the growth will be proportional to powers of Υ and even exponential in Υ . Thus, $\langle \beta \rangle Z_1^\perp$, ω_r , as well as Q can be very sensitive to the growth.

Simulations have been performed for the 4-cm and 13-cm muon bunches in a quasi-isochronous collider ring, with a betatron tune $\nu_\beta \sim 6.24$, interacting with a broadband impedance with $Q = 1$ and $Z_1^\perp = 0.1$ M Ω /m at the angular resonant frequency $\omega_r = 50$ GHz. Initially, a bunch is populated with a vertical Gaussian spread of $\sigma_y = 3$ mm and $y' = 0$ for all particles. There is no offset for the center of the bunch. Ten thousand macro-particles are used to represent the bunch containing 4×10^{12} beam particles. The half-triangular bin size is 15 ps (or 0.45 cm). In Fig. 15.3 we show the total growth of the *normalized* beam size $\sigma_y \equiv \langle y^2 + (\langle \beta \rangle y')^2 \rangle^{1/2}$ relative to the initial beam size up to

1000 turns for various values of $\langle\beta\rangle$, respectively, for the 13-cm and 4-cm bunches. The turn-by-turn decay of the muons has been taken into account. We see that the beam size grows very much faster for larger betatron function. Also the growths for the 4-cm bunch are much larger than those for the 13-cm bunch because the linear charge density of the former is larger.

15.2.1 Balakin-Novokhatsky-Smirnov Damping

Kim, Wurtele, and Sessler [2] suggested to suppress the growth of the transverse beam breakup by a small tune spread in the beam, coming either through chromaticity, amplitude dependency, or beam-beam interaction. This is because a beam particle will be resonantly driven by only a small number of particles in front that have the same betatron tune. This is a form of Balakin-Novokhatsky-Smirnov (BNS) damping suggested in 1983 [3].

To implement this, we add a detuning term

$$\Delta\nu_{\beta_i} = a[y_i^2 + (\langle\beta\rangle y_i')^2] \quad (15.15)$$

to the i th particle, as if it is contributed by an octupole or sextupole. In Fig. 15.4, we plot the growths of the normalized beam size relative to the initial beam size with various rms tune spreads $\sigma_{\nu_\beta} = a\langle\sigma_y^2 + (\langle\beta\rangle\sigma_{y'})^2\rangle$. Here, an average betatron function of $\langle\beta\rangle = 20$ m has been used. This is because BPMs, which contribute significantly to the transverse impedance, are usually installed at locations where the betatron function is large. We see in the top plot that to damp the growth of the 13-cm bunch to less than 1%, we need an rms tune spread of $\sigma_{\nu_\beta} = 0.0008$ or a total tune spread of $\Delta\nu_\beta = 3\sigma_{\nu_\beta} = 0.0024$. On the other hand, to damp the growth of the 4-cm bunch to less than 1%, we need (lower plot) an rms tune spread of $\sigma_{\nu_\beta} = 0.006$ or a total tune spread of $\Delta\nu_\beta = 3\sigma_{\nu_\beta} = 0.018$. We also see a saturation of the emittance growth for the 4-cm bunch. However, if the transverse impedance is larger, the average betatron function is larger, the resonant frequency is larger, or the quality factor is smaller, this required tune spread may become too large to be acceptable. This is because a large amplitude-dependent tune spread can lead to reduction of the dynamical aperture of the collider ring.

For the lattice of the muon collider ring designed by Trbojevic and Ng [1], in order to allow for a large enough momentum aperture, the amplitude-dependent tune shifts

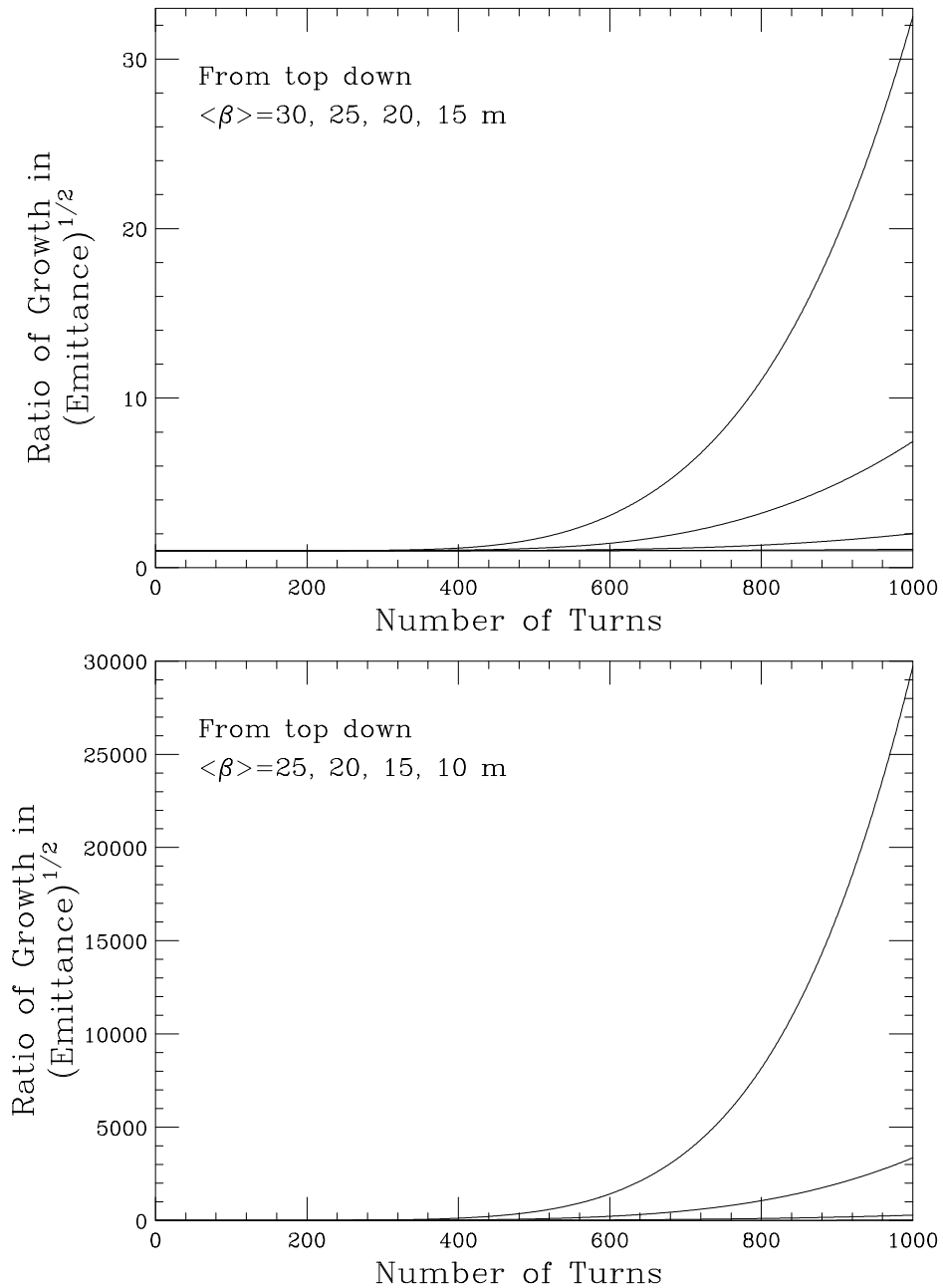


Figure 15.3: Beam-breakup growth for 1000 turns of a muon bunch interacting with a broadband impedance of $Q = 1$, $Z_1^\perp = 0.1 \text{ M}\Omega/\text{m}$ at the angular resonant frequency of $\omega_r = 50 \text{ GHz}$. Top: rms 13 cm bunch has total growths of 32.50, 7.4, 2.0, 1.09, 1.006, respectively for $\langle\beta\rangle = 30, 25, 20, 15, 10$ m. Bottom: rms 4 cm bunch has total growths of 29713, 3361, 287, 16.2, respectively for $\langle\beta\rangle = 25, 20, 15, 10$ m.

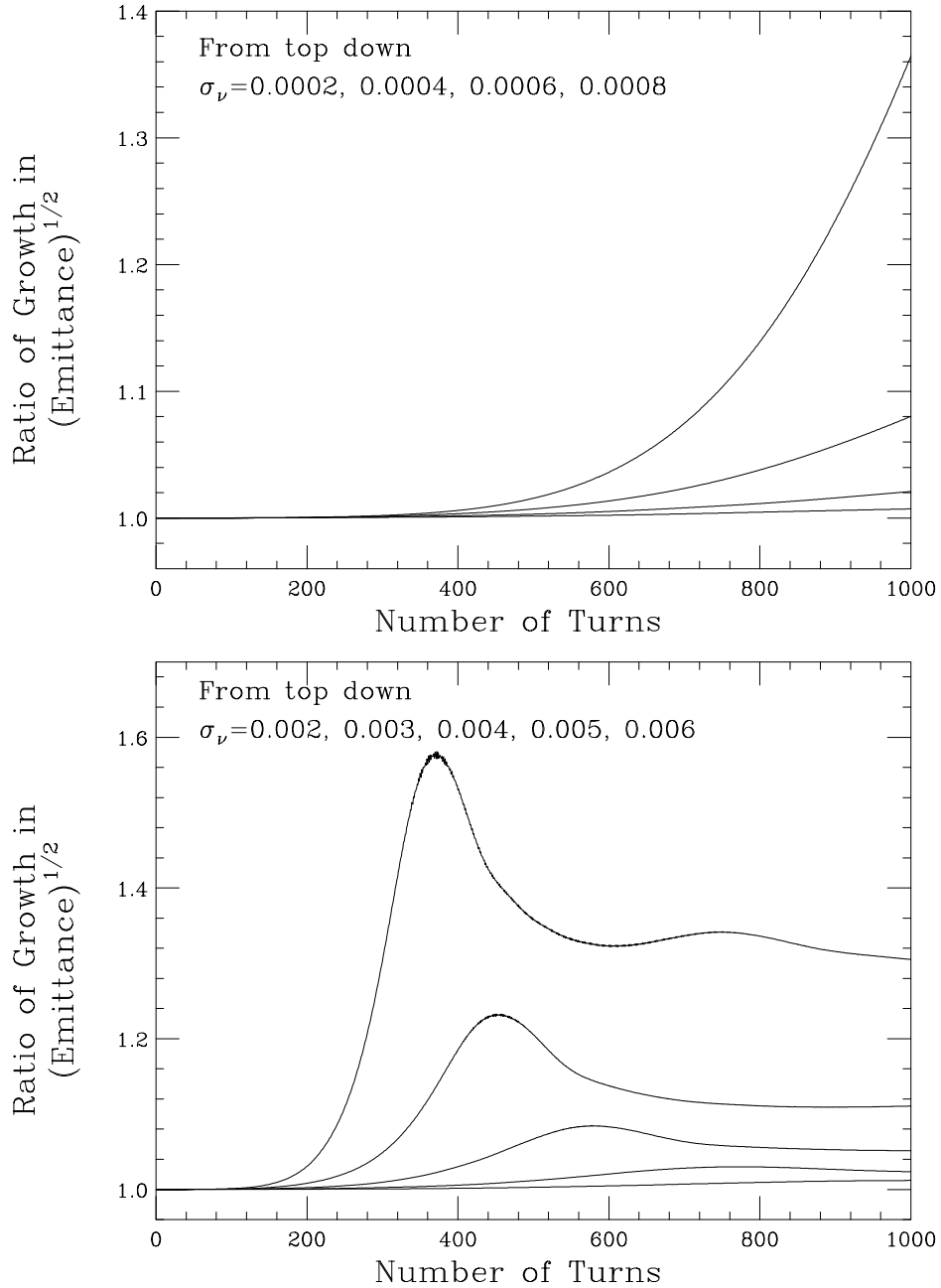


Figure 15.4: Total growth in 1000 turns in the presence of an amplitude dependent tune shift, such as provided by an octupole. An average betatron function of $\langle\beta\rangle = 20$ m has been assumed. Top: growths of the rms 13 cm bunch are 1.36, 1.08, 1.02, 1.007, respectively for rms tune spread of $\sigma_{\nu_\beta} = 0.0002, 0.0004, 0.0006, 0.0008$. Bottom: growths of the rms 4 cm bunch are 1.58, 1.23, 1.08, 1.03, 1.012, respectively for rms tune spread of $\sigma_{\nu_\beta} = 0.002, 0.003, 0.004, 0.005, 0.006$.

are

$$\begin{aligned}\nu_{\beta x} &= 8.126 - 100\epsilon_x - 4140\epsilon_y \\ \nu_{\beta y} &= 6.240 - 4140\epsilon_x - 50.6\epsilon_y\end{aligned}\tag{15.16}$$

for the on-momentum particles, where the unnormalized emittances ϵ_x and ϵ_y are measured in πm . For the 4-cm bunch, the normalized rms emittance is $\epsilon_{\text{Nrms}} = 85 \times 10^{-6} \pi\text{m}$. Since the muon energy is 50 GeV, the unnormalized rms emittance is $\epsilon_{\text{rms}} = 1.80 \times 10^{-7} \pi\text{m}$, and becomes $1.62 \times 10^{-6} \pi\text{m}$ when 3σ are taken. Thus, the allowable tune spread for the on-momentum particles is $\Delta\nu_\beta = 4140\epsilon_y = 0.0067$. Tune spreads larger than this will lead to much larger tune spreads for the off-momentum particles, thus reducing the momentum aperture of the collider ring. For 4-cm bunch, to damp beam breakup to about 1% when $Z_1^\perp = 0.1 \text{ M}\Omega/\text{m}$ and $\langle\beta\rangle = 20 \text{ m}$, one needs $\Delta\nu_\beta = 0.018$. However, we do not know exactly what $\langle\beta\rangle$ and Z_1^\perp are. Simulations show that if $\langle\beta\rangle Z_1^\perp$ becomes doubled, 2.5 times, 5 times, and 10 times, the tune spreads required jump to, respectively, $\sim 0.054, 0.073, 0.18, \text{ and } 0.54$. Thus, it appears that pure tune spread may be able to damp beam breakup for the 13-cm bunch but may not work for the 4-cm bunch. Although tune spreads due to chromaticity and beam-beam interaction will also damp beam breakup, it is unclear how much the momentum aperture will be reduced due to these tune spreads.

15.2.2 Autophasing

The transverse beam breakup can be cured by varying the betatron tune of the beam particles along the bunch, so that resonant growth can be avoided. In the two-particle model, if we allow

$$\Delta k_\beta = -\frac{e^2 N W_1(\hat{z})}{2L E_0 \bar{k}_\beta}\tag{15.17}$$

in Eq. (15.4), it appears that the linear increasing term will be eliminated and the tail particle motion

$$y_2(s) = y_{10} \cos \bar{k} s \cos \frac{\Delta k s}{2}\tag{15.18}$$

will be bounded. However, if we set

$$\Delta k_\beta = -\frac{e^2 N W_1(\hat{z})}{4L E_0 \bar{k}_\beta} = \frac{\Upsilon(\ell)}{\ell}\tag{15.19}$$

instead, the tail particle motion becomes

$$y_2(s) = y_{10} \left[\cos \bar{k}s \cos \frac{\Delta k_\beta s}{2} - \sin \bar{k}s \sin \frac{\Delta k_\beta s}{2} \right] = y_{10} \cos k_1 s , \quad (15.20)$$

which is exactly the same as the head particle. Being in phase all the time, the tail cannot be driven by the head at all. This is another form of BNS damping known as *autophasing* [4]. Exactly the same result will evolve if we solve Eq. (15.2) directly by enforcing $y_2(s) = y_1(s) = y_{10} \cos k_1 s$. Thus autophasing implies

$$\frac{\Delta k_\beta}{k_\beta} = \frac{\Upsilon}{\bar{k}_\beta \ell} . \quad (15.21)$$

For a particle-distributed bunch, in order that all particles will perform betatron oscillation with the same frequency and same phase after the consideration of the perturbation of the transverse wake, special focusing force is required to compensate for the variation of unperturbed betatron tune along the bunch. With the linear distribution $\rho(z)$, the equations of motion of Eq. (15.2) in the two-particle model generalize to

$$\frac{d^2 y(z, s)}{ds^2} + [k_\beta + \Delta k_\beta(z)]^2 y(z, s) = -\frac{e^2 N}{LE_0} \int_{-\infty}^z dz' \rho(z') W_1(z - z') y(z', s) , \quad (15.22)$$

where $z > 0$ denotes the tail and $z < 0$ the head, or the bunch is traveling towards the left. We need to choose the compensation $\Delta k_\beta(z)$ along the bunch in such a way that the betatron oscillation amplitude

$$y(z, s) \sim \sin(k_\beta s + \varphi_0) \quad (15.23)$$

is independent of z , the position along the bunch, with φ_0 being some phase, because only in this way any particle will not be driven by a resonant force from any particle in front. The solution is then simply

$$2k_\beta \Delta k_\beta + \Delta k_\beta^2(z) = -\frac{e^2 N}{LE_0} \int_{-\infty}^z dz' \rho(z') W_1(z - z') , \quad (15.24)$$

or, for small compensation $\Delta k_\beta(z)$,

$$\frac{\Delta k_\beta(z)}{k_\beta} = -\frac{e^2 N R}{2LE_0 k_\beta^2} \int_{-\infty}^z dz' \rho(z') W_1(z - z') . \quad (15.25)$$

If the linear bunch distribution $\rho(z)$ is a Gaussian interacting with a broadband impedance, the integration can be performed exactly to give

$$\frac{\Delta k_\beta(z)}{k_\beta} = \frac{e^2 N \omega_r^2 Z_1^\perp}{2LE_0 k_\beta^2 2\bar{\omega}Q} e^{-z^2/(2\sigma_t^2)} \mathcal{I}m w \left[\frac{ve^{i\phi_0}}{\sqrt{2}} - \frac{iz}{\sqrt{2}\sigma_\ell} \right], \quad (15.26)$$

where

$$w(z) = e^{-z^2} \left[1 + \frac{2i}{\sqrt{\pi}} \int_0^z e^{t^2} dt \right]. \quad (15.27)$$

is the complex error function while $\sin \phi_0 = 1/(2Q)$ and $v = \omega_r \sigma_\ell / c$ as defined in Eqs. (15.8) and (15.9). For long bunches and high resonant frequency, or $v \gg Q$, the complex error function behaves as

$$w(z) = \frac{i}{\sqrt{\pi}z} + \mathcal{O}\left(\frac{1}{|z|^3}\right). \quad (15.28)$$

This is certainly satisfied by both the 4-cm and 13-cm muon bunches, where $v = 6.67$ and 21.7, respectively, but not by the short electron bunches. Let us first discuss the long muon bunches in a storage ring. For convenience, we convert the betatron number to betatron tune by $k_\beta = \nu_\beta / R$ and the length L to the ring circumference $C = 2\pi R$. Thus Δk_β , the shift in betatron wave number in a cavity length L , becomes $\Delta \nu_\beta / R$, where $\Delta \nu_\beta$ is the betatron tune shift in a turn. Then, the relative tune shift compensation in Eq. (15.26) can be simplified to

$$\frac{\Delta \nu_\beta(z)}{\nu_\beta} \approx \frac{e^2 N \omega_r Z_1^\perp R}{2(2\pi)^{3/2} \nu_\beta^2 Q v E_0} \left[1 + \frac{z}{vQ\sigma_\ell} \right] e^{-z^2/(2\sigma_t^2)}. \quad (15.29)$$

This is the situation for the autophasing of the longer muon bunches, which is very different from the autophasing for the short electron bunches. The relative tune shift compensations required for the two long bunches are shown in the top plot of Fig. 15.5. Note that in Eq. (15.29), vQ controls the asymmetry of the tune shift compensation curve. When $vQ \rightarrow \infty$, there is no asymmetry and the compensation curve reduces to just a Gaussian, and, at the same time, $\Delta \nu_\beta / \nu_\beta$ decreases to zero. On the other hand, when $v \ll Q$ for short bunches or low broadband resonant frequency, the relative tune shift becomes rather linear as depicted by the 1.8 mm ($v = 0.3$) curve in the lower plot of Fig. 15.5. The curves for the 5.0 mm, 1.0 cm, and 4 cm bunch ($v = 0.83, 1.67,$ and 6.67) are also shown for comparison. Note that as the bunch length gets shorter, the frequency components of the tune compensation become much lower. For a very short bunch, the compensation becomes nearly linear in the region of the bunch.

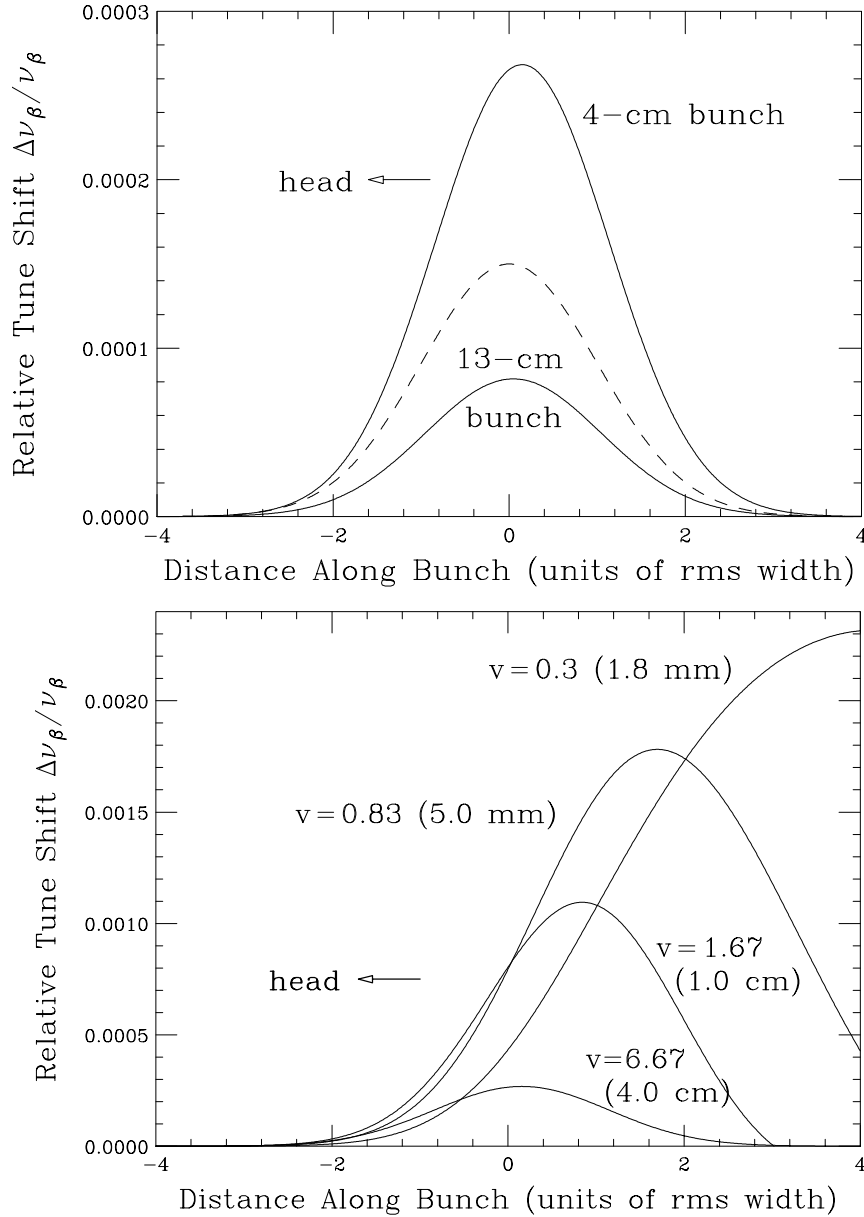


Figure 15.5: Relative tune shift autophasing compensation at distance z/σ_ℓ behind the bunch center (or bunch going to the left) to cure beam breakup. Impedance is broadband resonating at $\omega_r = 50$ GHz. Top: for the rms 4-cm and 13-cm bunches, where $v = \omega_r \sigma_\ell / c = 6.67$ and 21.7 respectively, with bunch profile plotted in dashes as a reference. Bottom: for short bunches, rms 1.8, 5.0, 10.0 mm, with $v = 0.3, 0.83, 1.67$, respectively. The curve for the 4-cm bunch is plotted as comparison. Note that when v is small, the compensation is of much lower frequencies.

To cure beam breakup with autophasing damping in an electron linac, the electron bunch is usually placed off the crest of the rf wave so that the head and tail of the bunch will acquire slightly different energies, and therefore slightly different betatron tunes through chromaticity. For muon bunches in the collider ring, however, this method cannot be used. If one insists on having autophasing, an rf quadrupole must be installed and pulsed according to the compensation curve for each bunch as the bunch is passing through it. The variation of a quadrupole field at such high frequencies is not possible at all. Another method is to install cavities that have dipole oscillations at these frequencies, which is not simple either. For this reason, autophasing for long bunches is not practical at all.

15.3 Linac

15.3.1 Adiabatic Damping

Let us come back to the short electron bunches in a linac. An expression was given in Eq. (15.6) for the deflection of the tail particle in the two-particle model. In a linac, the bunches are accelerated and the energy change of the beam particles cannot be neglected. The equations of motion of the head and tail macro-particles now become

$$\frac{1}{\gamma} \frac{d}{ds} \left(\gamma \frac{dy_1}{ds} \right) + k_\beta^2 y_1 = 0 , \quad (15.30)$$

$$\frac{1}{\gamma} \frac{d}{ds} \left(\gamma \frac{dy_2}{ds} \right) + k_\beta^2 y_2 = - \frac{e^2 N W_1(\hat{z})}{2L\gamma E_{\text{rest}}} y_1 , \quad (15.31)$$

where E_{rest} is the particle rest energy. The betatron wave number, which we have set to be the same for the two macro-particles, can have different dependency on energy. One way is to have k_β energy independent or the particle makes the same number of betatron oscillations per unit length along the linac. This is actually the operation of a synchrotron, where the quadrupole fields are ramped in the same way as the dipole field. If we further assume a constant acceleration

$$\gamma(s) = \gamma_i(1 + \alpha s) , \quad (15.32)$$

where γ_i is the initial gamma and α is a constant, the equation of motion of the head becomes

$$\frac{d}{du} \left(u \frac{dy_1}{du} \right) + \frac{k_\beta^2}{\alpha^2} u y_1 = 0 , \quad (15.33)$$

where $u = 1 + \alpha s$. Usually the acceleration gradient α is much slower than the betatron wave number k_β . For example, in the $L_0 = 3$ km SLAC linac where electrons are accelerated from $E_i = 1$ GeV to $E_f = 50$ GeV, $\alpha = 0.0163 \text{ m}^{-1}$, while the betatron wave number is $k_\beta = 0.06 \text{ m}^{-1}$. In that case, the solution is (Exercise 15.1)

$$y_1(s) = \frac{\hat{y}}{\sqrt{1 + \alpha s}} \cos k_\beta s, \quad (15.34)$$

which is obtained by letting $y_1 = A \cos k_\beta s$ with A a slowly varying function of u . In fact, Eq. (15.33) is the Bessel equation; Eq. (15.34) is just the asymptotic behavior of $y_1(s) = \hat{y} J_0[k_\beta(1 + \alpha s)/\alpha]$.

The equation of motion of the tail becomes

$$\frac{d}{du} \left(u \frac{dy_2}{du} \right) + \frac{k_\beta^2}{\alpha^2} u y_2 = -\frac{e^2 N W_1(\hat{z})}{2L E_i \alpha^2} \frac{\hat{y}}{\sqrt{u}} \cos k_\beta s. \quad (15.35)$$

To obtain the particular solution, we try $y_2 = D \sin k_\beta s / \sqrt{u}$ with D a slowly varying function of u^\dagger . The final solution is

$$y_2(s) = \frac{\hat{y}}{\sqrt{1 + \alpha s}} \left[\cos k_\beta s - \frac{e^2 N W_1(\hat{z})}{4L E_i \alpha k_\beta} \ln(1 + \alpha s) \sin k_\beta s \right]. \quad (15.36)$$

Noticing that $E_i \alpha \approx E_f / L_0$, the growth for the whole length L_0 of the linac is

$$\Upsilon = -\frac{e^2 N W_1(\hat{z}) L_0}{4k_\beta E_f L} \ln \frac{E_f}{E_i}. \quad (15.37)$$

This is to be compared with Eq. (15.6), where we gain here a factor of

$$\mathcal{F} = \frac{E_i}{E_f} \ln \frac{E_f}{E_i} \quad (15.38)$$

For the SLAC linac, this factor is $\mathcal{F} = 1/12.8 = 0.0782$, meaning that the tail will be deflected by 12.8 less with the acceleration. This effect is called *adiabatic damping*.

15.3.2 Detuned Cavity Structure

The dipole wake function of a cavity structure is given by

$$W_1(z) = -2 \sum_n K_n \sin \frac{2\pi \nu_n z}{c} e^{-\pi \nu_n z / (c Q_n)} \quad z > 0, \quad (15.39)$$

[†]One can also try $y_2 = D \sin k_\beta s$ with D a slowly varying function of u .

where K_n , ν_n , and Q_n are the kick factor, resonant frequency, and quality factor of the n th eigenmode in the structure, and the particle velocity has been set to c . The kick factor is defined as

$$K_n = \frac{\pi R_n \nu_n}{Q_n}, \quad (15.40)$$

with R_n being the dipole shunt impedance of the n th mode. To reduce beam break up, it is important to reduce this dipole wake function.

One way to reduce the dipole wake is to manufacture the cavity structure with cell dimension varying gradually so that each cell has a slightly different resonant frequency. In this case, the effect of the wake due to each individual cell will not add together and the wake of the whole structure will be reduced. Such a structure is called a *detuned cavity structure* [5].

Let us first study the short-range part of the dipole wake. The assumption that all the cells do not couple can be made, and the wake function of Eq. (15.39) can be considered as the summation of the wake due to each individual cell. Thus, K_n , ν_n , and Q_n become the kick factor, resonant frequency, and quality factor of the n th cell. Since the variation from cell to cell is small, the summation can be replaced by an integral

$$W_1(z) \approx -2 \int d\nu K \frac{dn}{d\nu} \sin \frac{2\pi\nu z}{c}. \quad (15.41)$$

Some comments are in order. First, the decays due to the quality factors have been neglected, because these are high- Q cavities and we are interested in the short-range wake only. Second, $K(dn/d\nu)$ is considered a function of ν and the normalization of $dn/d\nu$ is unity because $W_1(z)$ in Eq. (15.41) is referred to as the *dipole wake per cell*. Since $K(dn/d\nu)$ must be a narrow function centered about the average resonant frequency of the cells $\bar{\nu}$, the wake can be rewritten as

$$W_1(z) \approx -2 \mathcal{I}m \left[e^{2i\pi\bar{\nu}z/c} \int dx K(\bar{\nu} + x) \frac{dn}{d\nu}(\bar{\nu} + x) e^{2\pi i x z/c} \right], \quad (15.42)$$

with $\nu = \bar{\nu} + x$. We see that the wake consists of a rapidly varying part, oscillating at frequency $\bar{\nu}$, and a slowly varying part, the envelope, that is given by the Fourier transform of the function $K(dn/d\nu)$ after it has been centered about zero. For uniform frequency distribution with *full* frequency spread $\Delta\nu$, the wake is given by

$$W_1(z) \approx -2\bar{K} \sin \frac{2\pi\bar{\nu}z}{c} \frac{\sin(\pi\Delta\nu z/c)}{\pi\Delta\nu z/c}, \quad (15.43)$$

with \bar{K} the average value of K . If the frequency distribution is Gaussian with rms width σ_ν , then

$$W_1(z) \approx -2\bar{K} \sin \frac{2\pi\bar{\nu}z}{c} e^{-2(\pi\sigma_\nu z/c)^2} . \quad (15.44)$$

In this case, the envelope also rolls off as a Gaussian. It seems reasonable to expect that the proper Gaussian frequency distribution is near ideal in the sense of giving a rapid drop in the wake function for a given total frequency spread, and this is the motivation for choosing the Gaussian detuning.

Take the example of the Next Linear Collider (NLC). Consider a detuned structure with $N = 206$ cells. The central frequency is $\bar{\nu} = 15.25$ GHz. The detuned frequency distribution is Gaussian with $\pm 2.5\sigma_\nu$, where the rms spread σ_ν is chosen as 2.5% of $\bar{\nu}$. It is found that the average kick factor is $\bar{K} = 40$ MV/nC/m². The envelope of such a wake is shown in the top plot of Fig. 15.6. Notice that the wake function in fact does start from zero and has a first peak around 80 MV/nC/m² at $z \approx c/(4\bar{\nu}) = 4.91$ mm. It is important to point out that the dipole wake function defined in this way differs from our usual definition; it is equal to our usual W_1/L with $L = 1$ m. The designed rms bunch length is $\sigma_\ell = 0.150$ mm which is much less than the first peak. Therefore, the detuned structure will not help the single-bunch breakup at all. The bunch spacing is 42 cm in one scenario and 82 cm in another. At the location of the second bunch, the wake has dropped by more than two orders of magnitude. Thus, this lowering of the wake will definitely help the multi-bunch train beam breakup.

There are some comments on the wake depicted in the top plot of Fig. 15.6. First, the wake does not continue to drop as a Gaussian (the dashed curve) after about 0.4 m. Instead, it rises again having another peak around 4.2 m, although this peak is very much less than the first one. The main reason is due to the finite number of cells in the structure and the Gaussian distribution has been truncated at $\pm 2.5\sigma_\nu$. It is easy to understand the situation when we look at the uniform frequency distribution of Eq. (15.43). The envelope is dominated by the $\sin x/x$ term which gives a main peak at $x = 0$ and starts to oscillate after the first zero at $z = c/\Delta\nu$. Second, the coupling of the cells will nevertheless become important at some larger distance. Thus, the long-range part of the wake cannot be trusted at all. Bane and Gluckstern [5] used a circuit model with coupled resonators to give a more realistic computation of the long range wake. Later, Kroll, Jones, *et al.* [6] introduced four damping manifolds with four holes in the cells to carry away the dipole wave generated by the beam. Their final wake is shown in the bottom plot of Fig. 15.6. We see that the short-range part of the wake is almost

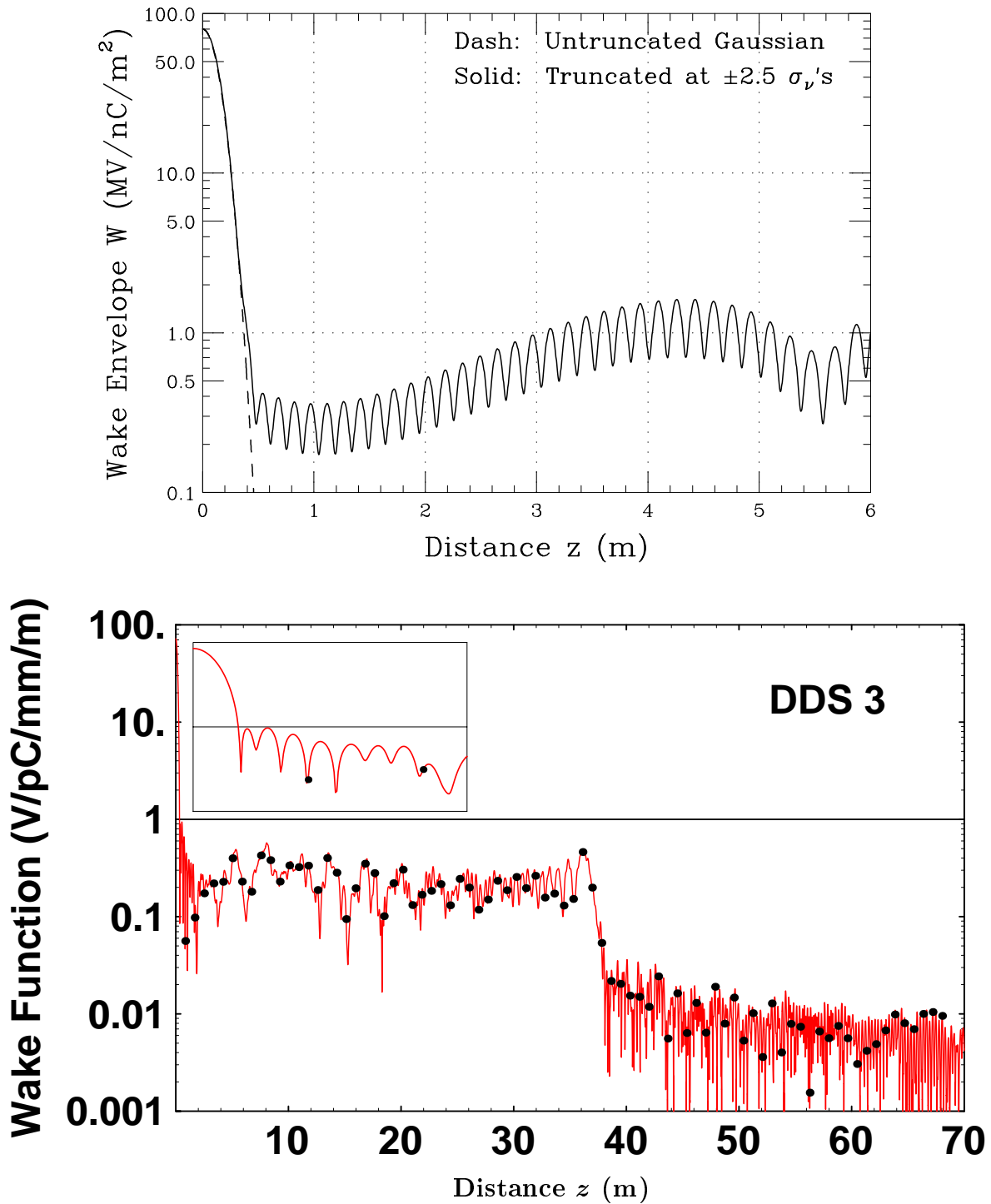


Figure 15.6: Envelope of the dipole wake function of a Gaussian detuned structure. Top: Coupling between cells has been ignored. Bottom: Coupling between cells has been included using a model with 2 circuits coupled to 4 manifolds. The dots represent the 82 bunches with 84-cm bunch spacing in one scenario.

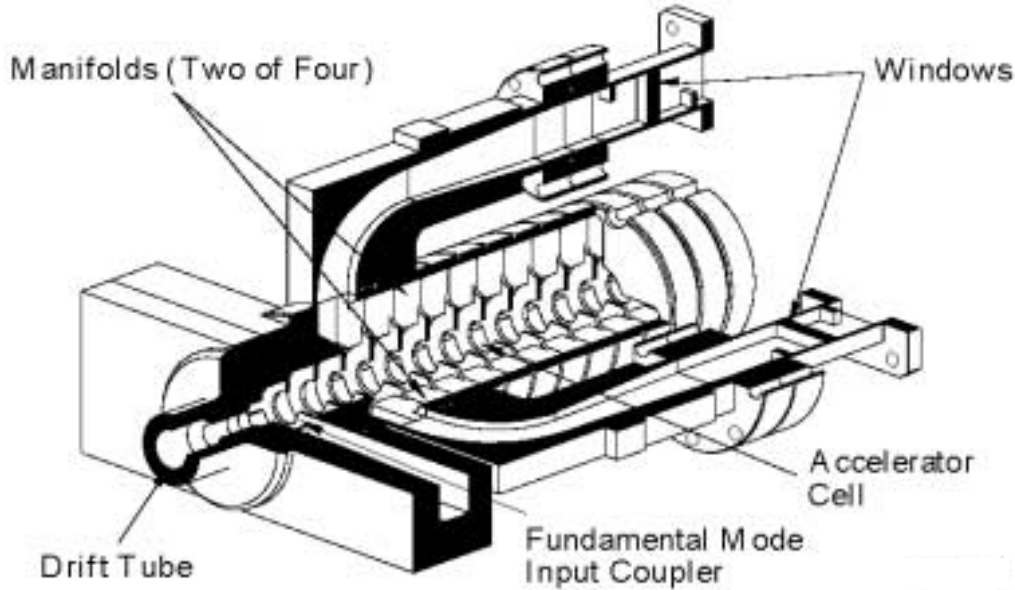


Figure 15.7: A drawing of the detuned structure consisting of 206 cavities coupled to 4 damped manifolds.

the same as is given by the top plot of Fig. 15.6. On the other hand, the long-range wake has been kept much below 1 MV/nC/m^2 . This wake has been computed first in the frequency domain as a spectral function and is then converted to the time or space domain via a Fourier transform. For this reason, we do not expect it to deliver the correct values at very short distances. The interested readers are referred to Refs. [5] and [6]. The dots on the plot represent the scenario of 82 bunches with 84-cm bunch spacing. A picture of the detuned structure consisting of 206 cavities coupled to four damped manifolds is shown in Fig. 15.7.

For the NLC, assuming a uniform energy independent betatron focusing with 100 betatron oscillations in the linac of total length $L = 10 \text{ km}$, the betatron wave number is $k_\beta = 0.06283 \text{ m}^{-1}$. Initially at 10 GeV, the NLC bunch has a vertical rms beam size of $\sigma_{y0} = 4.8 \text{ }\mu\text{m}$, or the effective normalized rms vertical emittance $\epsilon_y = 0.028 \text{ }\mu\text{m}$. At the linac exit (500 GeV), the deflection of the tail particle in the two-particle model is multiplied only $\Upsilon \sim 2.1$ fold per unit offset of the head particle (see Exercise 15.3). Assuming $1 \text{ }\mu\text{m}$ initial offset of the head particle, and conservation of normalized emittance in the absence of beam breakup, the normalized vertical emittance becomes $\epsilon_y = 0.30 \text{ }\mu\text{m}$. For

autophasing, assuming a chromaticity $\xi = 1$ defined by

$$\frac{\Delta k_\beta}{k_\beta} = \xi \delta , \quad (15.45)$$

an energy spread of 0.34% will be sufficient to damp the growth of the tail. These values are in close agreement of the simulations performed by Stupakov [10], as illustrated in Fig. 15.8.

15.3.3 Multi-Bunch Breakup

The NLC delivers a train of 95 bunches with bunch spacing 42 cm. Even if there is no beam breakup for a single bunch, the bunches in the train can also suffer beam breakup driven by the bunches preceding them. The first thing to do to ameliorate the situation is to design the linac cavities in such a way that the long-range dipole wake function will be as small as possible. The Gaussian detuned structure has been a way to lower the dipole wake by as much as two orders of magnitudes. According to the lower plot of Fig. 15.6, at 42 cm, the dipole wake is only ~ 0.21 MV/nC/m².

The two-particle model can be extended to accommodate the study of multi-bunch beam breakup. Each bunch is visualized as a macro-particle containing N electrons. Then the equation governing the displacement of the first bunch is

$$\frac{d^2 y_1}{ds^2} + k_\beta^2 y_1 = 0 , \quad (15.46)$$

and that of the second bunch is

$$\frac{d^2 y_2}{ds^2} + k_\beta^2 y_2 = -\frac{e^2 N W_1(\hat{z})}{LE} y_1 , \quad (15.47)$$

where L is the cavity length and W_1 is the transverse wake per cavity. The first equation is the free betatron oscillation and is the same as Eq. (15.1). The second equation differs slightly from Eq. (15.2) in not having the factor 2 in the denominator. This is because in the two-particle model of a bunch, each macro-particle contains $\frac{1}{2}N$ electrons and here each macro-particle represents one bunch which is composed of N electrons. Also the dipole wake $W_1(\hat{z})$ in Eq. (15.47) is evaluated at the bunch spacing \hat{z} . Recall that the two-particle model will not work when the bunch length is too long and falls out of the linear region of the dipole wake, because some particles in between the head and the tail

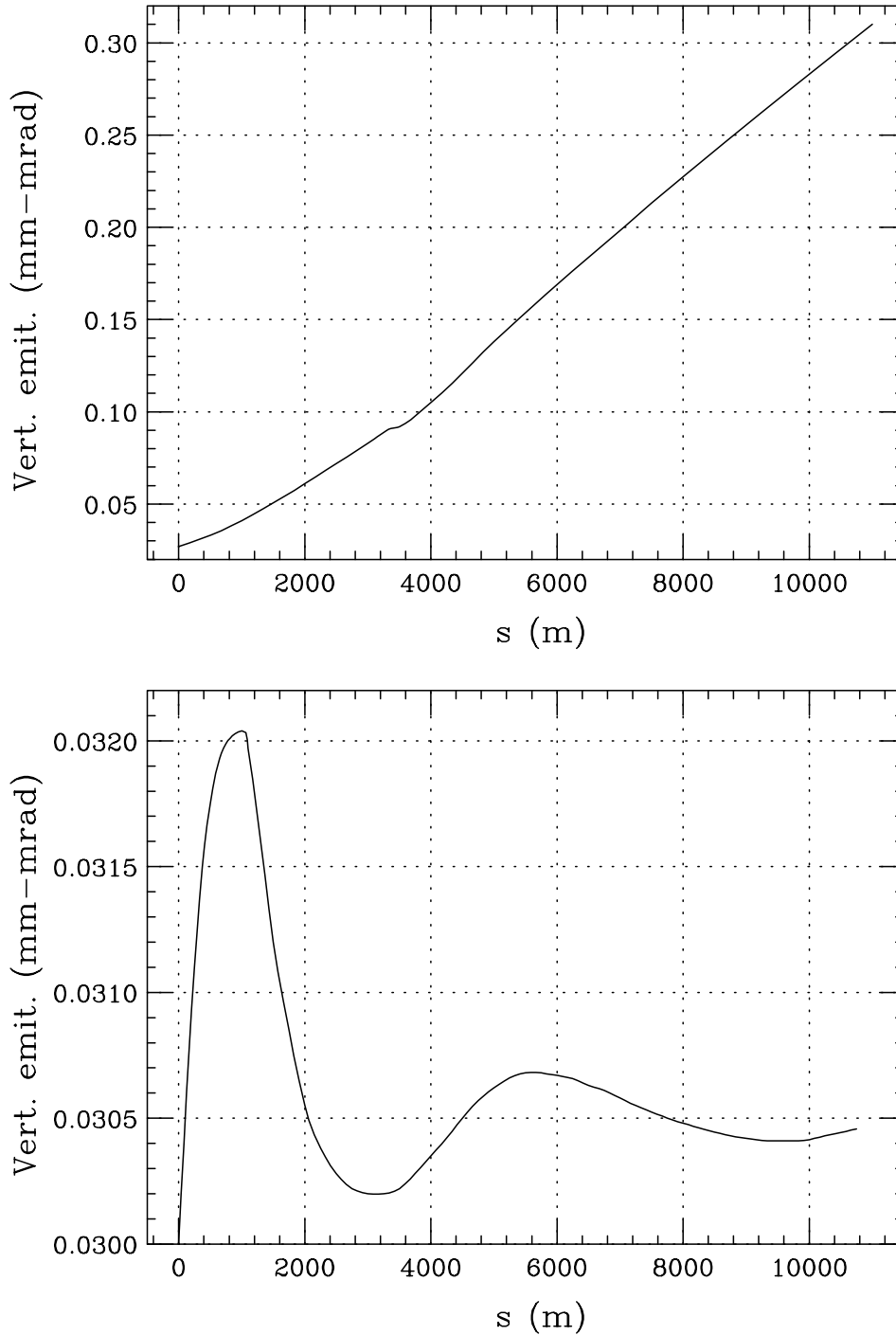


Figure 15.8: The normalized vertical emittance of a NLC bunch from the beginning to the end of the main linac, assuming an initial vertical offset of $1 \mu\text{m}$. Top: The emittance increases to $\sim 0.3 \mu\text{m}$ because of beam breakup. Bottom: An energy spread of $\sim 0.8\%$ is added across the bunch by offsetting the rf phase. The emittance increase has been damped.

will suffer more beam-breakup deflections than the tail. However, this model still works for a long train of bunches, because unlike a long bunch, there are no particles between the point bunches.

Now the solution for the first bunch is

$$y_1(s) = \mathcal{R}e \hat{y} e^{ik_\beta s} . \quad (15.48)$$

The solution for the second bunch is

$$y_2(s) = \mathcal{R}e \hat{y} \Gamma s e^{ik_\beta s} , \quad (15.49)$$

where

$$\Gamma = \frac{ie^2 N W_1(\hat{z})}{2k_\beta L E_0} , \quad (15.50)$$

and we have neglected the general solution

$$y_2(s)|_{\text{general}} = \hat{y} e^{\pm ik_\beta s} , \quad (15.51)$$

which is much smaller than the particular solution in Eq. (15.49) which grows linearly as s . The equation for the deflection of the third bunch is

$$\frac{d^2 y_3}{ds^2} + k_\beta^2 y_3 = -\frac{e^2 N W_1(2\hat{z})}{L E_0} y_1 - \frac{e^2 N W_1(\hat{z})}{L E_0} y_2 . \quad (15.52)$$

Here, we are going to retain only the largest driving force on the right-side. This means that the driving force from y_1 can be neglected and so is the force from the general solution of y_2 . Substituting Eq. (15.49) in Eq. (15.52), we solve for the most divergent solution

$$y_3(s) = \mathcal{R}e \hat{y} \frac{1}{2} \Gamma^2 s^2 e^{ik_\beta s} . \quad (15.53)$$

Continuing this way, the deflection for the m th bunch will be (Exercise 15.4)

$$y_m(s) = \mathcal{R}e \hat{y} \frac{1}{(m-1)!} \Gamma^{m-1} s^{m-1} e^{ik_\beta s} . \quad (15.54)$$

Stupakov [11] tries to estimate how much energy spread will be required to BNS damp the multi-bunch beam breakup. In order to damp the deflection of the second bunch, the amount of tune spread is

$$\frac{\Delta k_\beta}{k_\beta} = -\frac{e^2 N W_1(\hat{z})}{2k_\beta^2 E_f} \ln \frac{E_f}{E_i} , \quad (15.55)$$

taking the linac acceleration into account. It is reasonable to assume that n_b times the spread necessary for the second bunch will be required for n_b bunches. Next the natural chromaticity for a FODO lattice of phase advance μ is

$$\xi = -\frac{2}{\pi} \tan \frac{\mu}{2} . \quad (15.56)$$

For 95 bunches, one gets the required energy spread of 2.7% (Exercise 15.5). The simulations by Stupakov are shown in Fig. 15.9. The initial bunch offset is $1 \mu\text{m}$ and it takes an rms energy spread of 0.8% among the bunches to damp the growth.

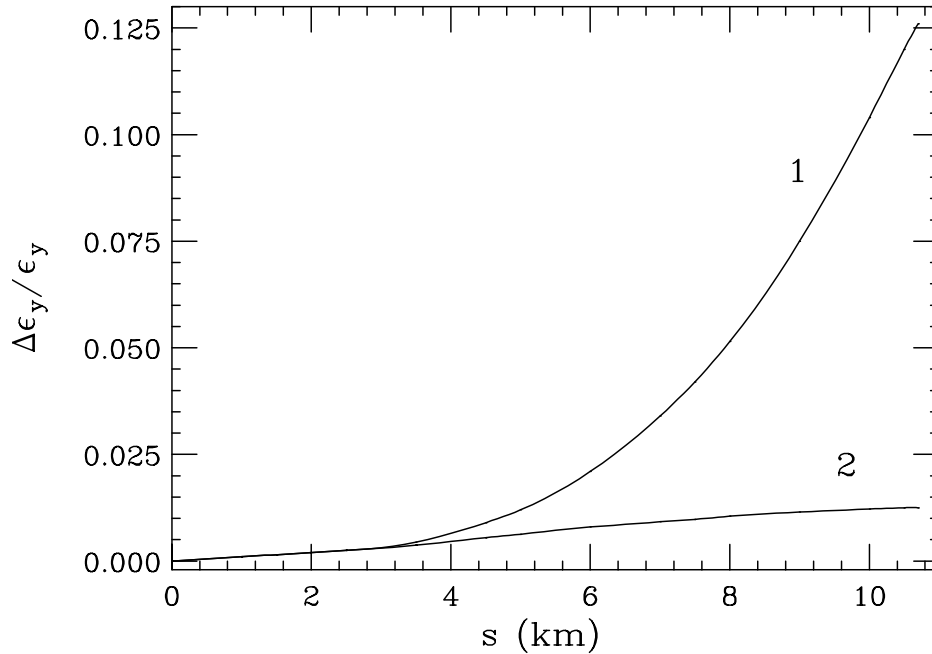


Figure 15.9: The relative change in vertical emittance of the 95th bunch, taking the vertical size as the vertical offset of the bunch center added to the actual rms vertical size in quadrature. The initial vertical offset is $1 \mu\text{m}$. Curve 1 shows the growth without any energy variation in the bunches. Curve 2 shows that the beam-breakup growth has been damped with a 0.8% rms energy spread varying linearly from the first to the 95th bunch.

15.3.4 Analytic Treatment

Analytic computation of beam breakup for a bunch train has been attempted by many authors [8, 7]. In all these papers, the dipole wake has been taken as a single dipole

resonance and BNS damping has not been included. Recently, Bohn and Ng [9] have been able to include an energy chirp and derive analytic expressions for the BNS damping of a train of point bunches. Essentially, the energy chirp gives rise to a spread in betatron wave number among the bunches. An outline of the analytic derivation is given below.

Introduce the dimensionless *spatial* parameter $\sigma = s/L_0$ normalized to the total linac length L_0 . The real time t is reduced to the dimensionless *time* parameter $\zeta = \omega_r(t - s/c)$, with ω_r being the dipole resonant angular frequency, to describe the arrival of the a particle of the beam at position s along the linac, with $\zeta = 0$ as the arrival time of the first particle. Thus, ζ measures the longitudinal position of the particle inside the beam. The transverse displacement of a particle in the beam, represented by $y(\sigma, \zeta)$, depends on both σ and ζ and its motion is governed by[‡]

$$\left[\frac{1}{\gamma} \frac{\partial}{\partial \sigma} \left(\gamma \frac{\partial}{\partial \sigma} \right) + \kappa^2(\sigma, \zeta) \right] y(\sigma, \zeta) = -\epsilon(\sigma) \int_0^\zeta d\zeta' w(\zeta - \zeta') F(\zeta') y(\sigma, \zeta') , \quad (15.57)$$

which is just another way of writing Eq. (15.14) with beam particle acceleration included as in Eq. (15.31). This equation is usually referred to as the multi-bunch cumulative beam breakup (MBBU) equation. Here, the normalized betatron wave number is $\kappa = k_\beta L_0$. The beam profile $F(\zeta)$ will be defined in Eq. (15.60) below. The normalized dipole wake is[§]

$$w(\zeta) = -H(\zeta) e^{-\zeta/(2Q)} \sin \zeta , \quad (15.58)$$

where Q is its quality factor and $H(\zeta)$ is the Heaviside step function. All the rest is lumped into the dimensionless beam-breakup coupling strength

$$\epsilon(\sigma) = \frac{e^2 N w_0 L_0^2}{\gamma E_{\text{rest}} \omega_r \tau} , \quad (15.59)$$

where w_0 is the sum-wake amplitude or twice the kick factor of the dipole resonance measured in V/C/m² and $N/(\omega_r \tau)$ is the number of electrons per *longitudinal time* ζ . For a train of bunches with temporal spacing τ , N becomes the number per bunch. When these bunches are further considered as points, the beam profile in above is represented by

$$F(\zeta) = \sum_{n=-\infty}^{\infty} \delta \left(\frac{\zeta}{\omega_r \tau} - n \right) . \quad (15.60)$$

[‡]The arrival time is $\xi = 0$ for the first particle and $\xi > 0$ for later particles, or it represents a arrival time *behind* the first particle.

[§]This is another convention of defining the transverse wake so that it increases with a positive slope at the beginning. This is also called the *sum wake* because it represents the sum of the wake fields left by all preceding particles.

All bunches with arrival time $\zeta < 0$ will be excluded by the causal property of the wake.

A betatron linear chirp is now introduced,

$$\kappa(\sigma, \zeta) = \kappa_0(\sigma) + \kappa_1(\sigma, 0)\zeta, \quad (15.61)$$

where $\kappa_0(\sigma)$ is the normalized betatron wave number without the chirp and $\kappa_1(\sigma, 0)$ represents the strength of a linear chirp across the bunches. With the assumption that the acceleration gradient is much less than the betatron wave number, we can introduce a new transverse offset variable

$$\xi(\sigma, \zeta) = \sqrt{\gamma(\sigma)} y(\sigma, \zeta) e^{-i\zeta\Delta(\sigma)}, \quad (15.62)$$

where $\Delta(\sigma) = \int_0^\sigma d\sigma' \kappa_1(\sigma', 0)$. Now Eq. (15.57) can be rewritten as[¶]

$$\left[\frac{\partial^2}{\partial \sigma^2} + \kappa_0^2(\sigma) \right] \xi(\sigma, \zeta) \simeq -\epsilon(\sigma) \int_0^\zeta d\zeta' w_\Delta(\sigma, \zeta - \zeta') F(\zeta') \xi(\sigma, \zeta'), \quad (15.63)$$

where the assumption of strong focusing, $\partial\xi(\sigma, \zeta)/\partial\sigma \simeq i\kappa_0\xi(\sigma, \zeta)$, has been used. Strong focusing actually implies that the quadrupole focusing is the most important force, while the wake, the acceleration gradient, and the variation of focusing due to chirping are small. The chirped-modified wake in Eq. (15.63) is defined as

$$w_\Delta(\sigma, \zeta) = w(\zeta) e^{-i\zeta\Delta(\sigma)}, \quad (15.64)$$

where obviously the exponential comes from the definition of $\xi(\sigma, \zeta)$. This exponential, when combined with the exponential of the original wake of Eq. (15.58), gives an *effective quality factor* Q_{eff} , where

$$\frac{1}{2Q_{\text{eff}}} = \frac{1}{2Q} + i\Delta. \quad (15.65)$$

Immediately, a result can be drawn that the chirp will be important if the quality factor Q of the transverse wake is high, but will be masked if Q is sufficiently low.

The transformation into Eq. (15.63) is important, because the operator on the left side no longer depends on ζ , and the chirp has been incorporated into the dipole wake. To proceed, we Fourier transform the whole equation with respect to the variable $\xi = n\omega_r\tau$ to obtain

$$\left[\frac{\partial^2}{\partial \sigma^2} + \kappa_0^2(\sigma) \right] \tilde{\xi}(\sigma, \theta) \simeq -\epsilon(\sigma) \omega_r \tau \tilde{w}_\Delta(\sigma, \theta) \tilde{\xi}(\sigma, \theta), \quad (15.66)$$

[¶] $(\gamma')^2$ and γ'' will be neglected in below, where the prime implies derivative with respect to σ , but $\gamma'\xi'$ will be retained.

where

$$\begin{aligned}\tilde{\xi}(\sigma, \theta) &= \sum_{m=0}^{\infty} e^{-im\theta} \xi(\sigma, m\omega_r\tau) , \\ \tilde{w}_\Delta(\sigma, \theta) &= \sum_{m=0}^{\infty} e^{-im[\theta+\omega_r\tau\Delta(\sigma)]} w_m = w(\sigma, m\omega_r\tau) .\end{aligned}\quad (15.67)$$

In this form, the WKB method can be employed to give a formal solution

$$\tilde{\xi}(\sigma, \theta) = \sqrt{\frac{\Lambda(0, \theta)}{\Lambda(\sigma, \theta)}} \exp \left[i \int_0^\sigma d\sigma' \Lambda(\sigma', \theta) \right] , \quad (15.68)$$

where

$$\Lambda^2(\sigma, \theta) = \kappa_0^2(\sigma) + \epsilon(\sigma)\omega_r\tau\tilde{w}_\Delta(\sigma, \theta) . \quad (15.69)$$

Here $\Lambda(\sigma, \theta)$ is an auxiliary function reflecting the coupling between the bunch spacing and the deflecting-mode frequency, and when $\tilde{w}_\Delta(\sigma, \theta)$ is substituted, it takes the form

$$\Lambda(\sigma, \theta) = \kappa_0(\sigma) \left[1 - \frac{\epsilon(\sigma)}{4\kappa_0^2(\sigma)} \frac{\omega_r\tau \sin \omega_r\tau}{\cos[\theta+\omega_r\tau\Delta(\sigma)] - \cos \omega_r\tau} \right] . \quad (15.70)$$

Denoting the displacement for the $(m+1)$ th bunch as $y_m(\sigma) = y(\sigma, m\omega_r\tau)$, the inverse Fourier transform give [8, 12]

$$y_m(\sigma) = \frac{1}{2\pi} \sum_{n=0}^m e^{-n\omega_r\tau/(2Q)} \int_{-\pi}^{\pi} d\theta e^{-in\theta} \left\{ y_{m-n}(0) \mathcal{C}(\sigma, \theta; m) + y'_{m-n}(0) \frac{\mathcal{S}(\sigma, \theta; m)}{\Lambda(0, \theta)} \right\} , \quad (15.71)$$

in which

$$\left\{ \begin{array}{l} \mathcal{C}(\sigma, \theta; m) \\ \mathcal{S}(\sigma, \theta; m) \end{array} \right\} = \sqrt{\frac{E_i \Lambda(0, \theta)}{E_\sigma \Lambda(\sigma, \theta)}} \left\{ \begin{array}{l} \mathcal{R}e \\ \mathcal{I}m \end{array} \right\} \exp \left[im\omega_r\tau\Delta(\sigma) + \int_0^\sigma d\sigma' \Lambda(\sigma', \theta) \right] \quad (15.72)$$

are cosine-like and sine-like functionals, respectively. In above, we have written, for convenience, the energy of the beam particle at location σ as $E_\sigma = \gamma(\sigma)E_{\text{rest}}$ and the initial energy as $E_i = \gamma(0)E_{\text{rest}}$. Later we will also write the energy at linac exit as $E_f = \gamma(1)E_{\text{rest}}$.

It is evident from Eq. (15.71) that upon taking $\theta \rightarrow -\theta$ and remembering that y_m is real, the algebraic sign of $\Delta(\sigma)$ affects only the phase of $y_m(\sigma)$ but not the envelope. This demonstrates that, as expected intuitively, the effect of a linear increase in focusing from head to tail is the same as a linear decrease.

In order for the derivation to go through analytically further, it is necessary to make the assumption that the betatron wave number decreases as $\gamma^{-1/2}$. This focusing arrangement implies that all the quadrupoles are identical and they can be on one common bus, because the focusing field gradient will be exactly the same along the linac. This implies the focusing becomes weaker as the energy increases. In fact, the NLC quadrupoles are deployed roughly in this way, although the quadrupoles there are all on separate buses for the ease of beam alignment. With this assumption, $\epsilon(\sigma)/[4\kappa_0^2(\sigma)]$ in the defining equation of $\Lambda(\sigma, \theta)$ above will no longer be dependent on σ . This simplifies the integration to be performed later.

For further discussion, let us set the initial conditions $y_m(0) = y_0$ and $y'_m(0) = 0$ for every bunch, and assume a constant acceleration gradient in the linac. The sum in Eq. (15.71) can be decomposed into two parts: $\sum_0^m = \sum_0^\infty - \sum_m^\infty$. The first part pertains to the *steady-state* displacement y_{ss} that would arise were the deflecting wake first seeded with an infinitely long bunch train immediately preceding the actual bunch train. Given strong focusing, the steady-state displacement is

$$y_{ss}(\sigma, m\omega_r\tau) \simeq y_0 \left[\frac{E_i}{E_\sigma} \right]^{1/4} \cos \left[m\omega_r\tau\Delta(\sigma) + \int_0^\sigma d\sigma' \kappa_0(\sigma') \right]. \quad (15.73)$$

The second part pertains to the *transient* displacement $\delta y_m = y_m - y_{ss}$. Saddle-point integration gives a closed-form solution for δy_m , whose bounding envelope takes the form:

$$\frac{|\delta y_m|}{y_0} \simeq \left[\frac{E_i}{E_\sigma} \right]^{1/4} \frac{\sqrt{\mathcal{E}} \exp[q(\eta)\mathcal{E} - m\omega_r\tau/(2Q)]}{4m\sqrt{2\pi} |\sin(\omega_r\tau/2)|} \times \begin{cases} |1 - \eta^2|^{-1/4} & \eta \text{ not near } 1 \\ \left(\frac{4}{3}\right)^{1/6} \mathcal{E}^{1/6} \frac{\Gamma(\frac{1}{3})}{\sqrt{2\pi}} & \eta = 1. \end{cases} \quad (15.74)$$

The auxiliary relations comprising Eq. (15.74) are:

$$\mathcal{E}(\sigma, m) = \left[\frac{4m\omega_0 e^2 N L_0^2}{\bar{\kappa}_0 E_i} \right]^{1/2} \frac{\left[\left(\sqrt{E_f/E_i} - 1 \right) \left(\sqrt{E_\sigma/E_i} - 1 \right) \right]^{1/2}}{E_f/E_i - 1},$$

$$\eta(\sigma, m) = \frac{\bar{\kappa}_0 |f_\gamma|}{2\mathcal{E}} \frac{m}{M} \frac{\sqrt{E_\sigma/E_i} - 1}{\sqrt{E_f/E_i} - 1},$$

$$q(\eta) = \begin{cases} \frac{\sqrt{1-\eta^2}}{2} + \frac{1}{4\eta} \tan^{-1} \left(\frac{2\eta\sqrt{1-\eta^2}}{1-2\eta^2} \right) & \eta < 1 \\ \frac{\pi}{4\eta} & \eta \geq 1, \end{cases}$$

in which $\bar{\kappa}_0$ is the focusing strength averaged over the linac and is related to the focusing strength at entrance $\kappa_0(0)$ by

$$\bar{\kappa}_0 = \frac{2\kappa_0(0)}{\sqrt{E_f/E_i + 1}}, \quad (15.76)$$

M is the total number of bunches in the train, $|f_\gamma|$ is the magnitude of the total fractional energy spread across the bunch train, or twice the total fractional focusing variation.

The expression for $|\delta y_m|$ in Eq. (15.74) reflects a number of physical processes. The coefficient involving beam energy manifests adiabatic damping. The factor $|\sin(\omega_r \tau/2)|$ is a relic of a resonance function deriving from the coupling between the bunch spacing and the deflecting-mode frequency. Resonances lie near even-order wake zero-crossings [8]; because the solution is valid only away from zero-crossing, resonance is removed. The focusing variation represented by $|f_\gamma|$ regulates exponential growth, and finite Q yields exponential damping. Yet “ $\eta=1$ ” does have special physical significance; it demarks the onset of saturation of exponential growth and, with infinite Q , algebraic decay of the envelope. For $\eta \geq 1$ the “growth factor” $q(\eta)\mathcal{E}$ is independent of bunch number m and of linac coordinate σ ; temporal “damping” then ensues through a negative power of m , and spatial “damping” ensues adiabatically as already mentioned. Therefore $\eta = 1$ corresponds to a global maximum in the envelope $|\delta y_m|$. The effect of the focusing variation is the saturation of the exponential growth, not damping; its action distinctly differs from that of a real effective Q .

We now apply the solution to designs of the SLAC NLC and DESY TESLA. Some parameters are listed in Table 15.1.

15.3.5 Amount of Energy Chirp

The transient displacements of the 90 bunches of the NLC at the linac exit were simulated and shown in Fig. 15.10 for energy spreads $f_\gamma = 1.5$ and 3.0%. The plots are made with the scenario that the linac is $L_0 = 10$ km long, accelerating 90 bunches with bunch spacing $\tau = 2.8$ ns from 10 GeV to 1 TeV. Each bunch contains 1 nC of charges or

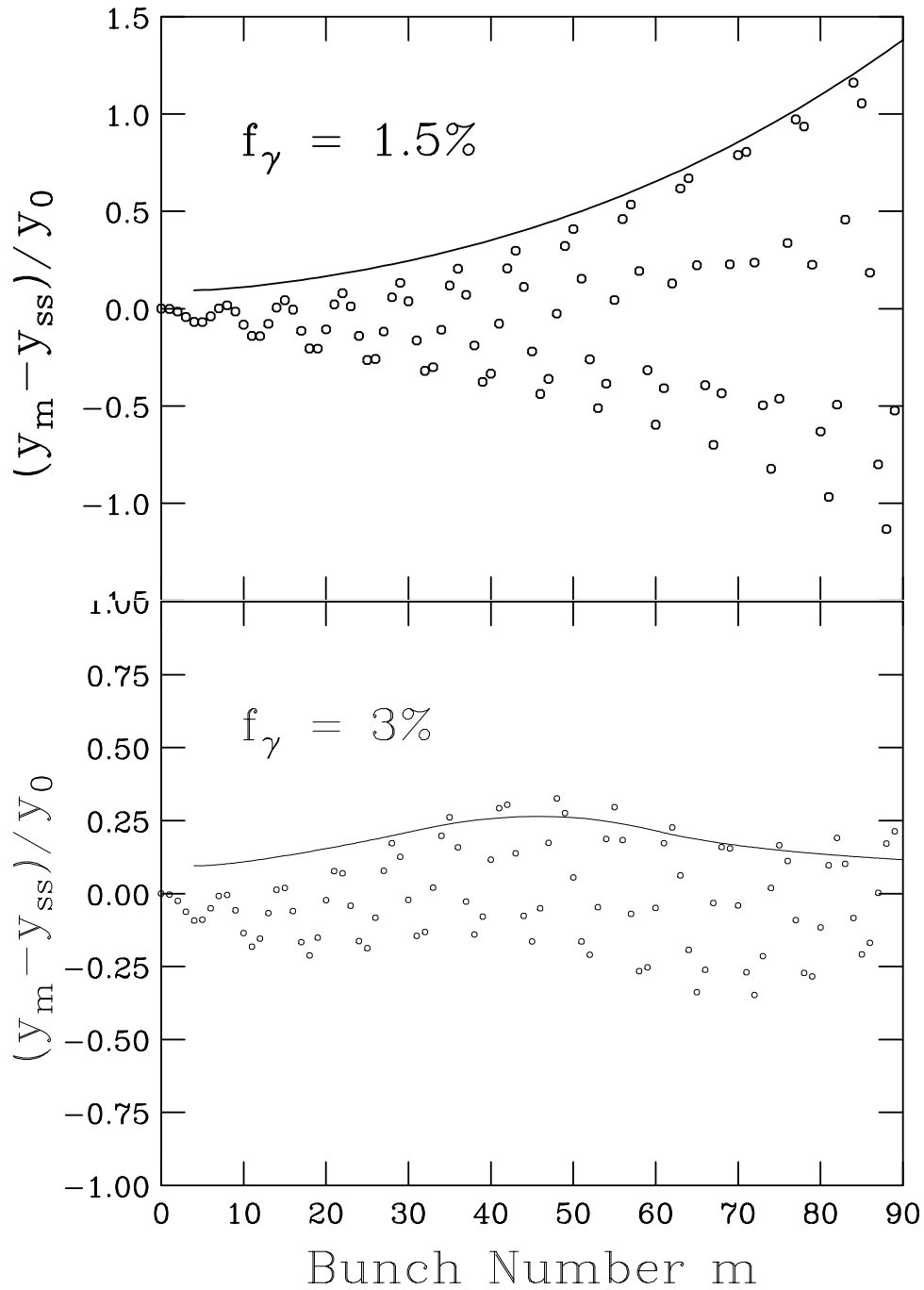


Figure 15.10: Analytic envelope at the linac exit (solid curve) plotted against the transverse displacement of bunches calculated numerically, with total energy spreads of 1.5% (top) and 3% (bottom).

Table 15.1: Some parameters of the SLAC NLC and DESY TESLA.

	NLC[†]	TESLA
Linac length ℓ (km)	10.0	14.4
No of betatron wavelengths ν_β	100	60
Entry/exit energy (GeV)	10/1000	5/250
No of bunches per train M	90	2820
Bunch charge q (nC)	-1.0	-1.6
Bunch spacing τ (ns)	2.8	377
Transverse wake:		
amplitude w_0 (V/pC/m/mm)	1	0.015
frequency $\omega_r/(2\pi)$ (GHz)	14.95	1.70
effective quality factor Q	∞	~ 125000
[†] The above belong to an older model of the SLAC NLC, and are chosen to illustrate MBBU. The parameters w_0 and Q represent a worst-case wake.		

$N = 6.24 \times 10^9$ electrons, making 100 betatron oscillations along the linac. The dipole wake of the SLAC NLC cavities is of resonant frequency $\omega_r/(2\pi) = 14.95$ GHz. Its long-range transverse behavior is shown in Fig. 15.6, which is computed using a circuit model. We see that the envelope of the wake is almost constant for the first 30 m or the first 36 bunch spacings. This allows us to assign an effective quality factor of $Q = \infty$ and sum-wake amplitude^{||} $w_0 \sim 1$ MV/nC/m². It is clear that BNS damping is helping to control the emittance growth. The relative displacement of the 90th bunch would be as large as 2.1 when $f_\gamma = 0$. We also see that with $f_\gamma = 3.0\%$ the envelope reaches a maximum at the 48th bunch and decays algebraically afterward approaching steady state slowly. An effective BNS damping requires an energy spread sufficient to have the maximum to reach some bunches before they leave the linac.

The special significance of $\eta = 1$ translates into a criterion for the focusing variation to be effective. Specifically, one should choose a value of f_γ that ensures $\eta(1, M) > 1$, *i.e.*, that $\eta = 1$ is reached somewhere along the bunch train before it leaves the linac.

^{||}The plot in Fig. 15.6 shows $w_0 \sim 0.3$ MV/nC/m². Here, we use $w_0 \sim 1$ MV/nC/m² as a reference model.

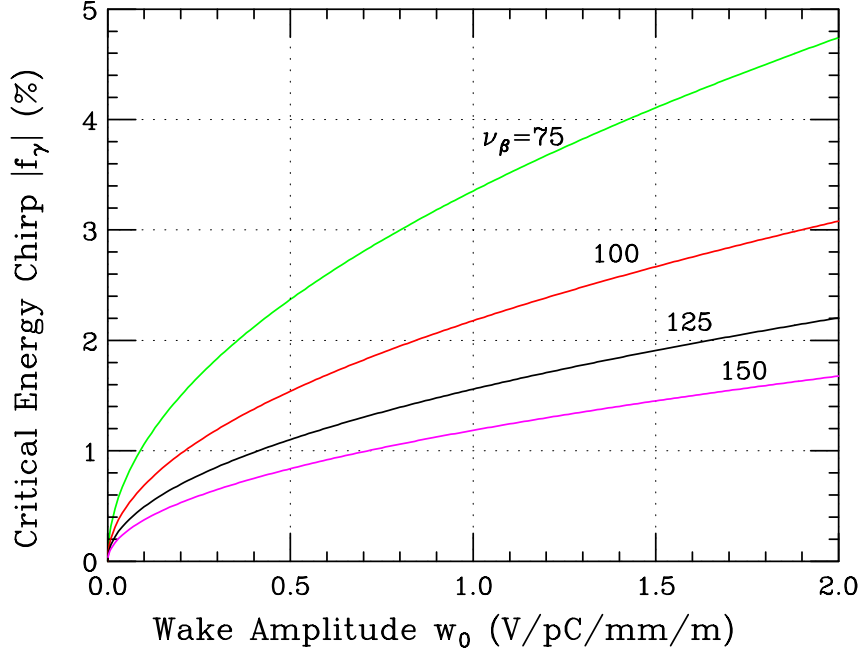


Figure 15.11: (color) Critical energy chirp required for BNS damping in the SLAC NLC versus deflecting wake amplitude, with number of betatron wavelengths $\nu_\beta = 75, 100, 125,$ and 150 .

According to the auxiliary relations to Eq. (15.74), the criterion is

$$|f_\gamma| > \frac{2\mathcal{E}(1, M-1)}{\bar{\kappa}_0} = \frac{\mathcal{E}(1, M-1)}{\pi\nu_\beta}, \quad (15.77)$$

which is plotted in Fig. 15.11 versus the wake amplitude for various strength of betatron focusing. For example, for the parameters in Table 15.1, an energy chirp of $|f_\gamma| \gtrsim 2.18\%$ in the NLC will be required. However, as will be seen in the next subsection, this is not the only criterion to control emittance growth.

15.3.5.1 Emittance Growth

The steady-state and transient displacements, being uncorrelated, comprise a measure of the total projected normalized emittance as

$$\varepsilon \equiv (|y_{ss}|^2 + |\delta y_m|_{max}^2) \frac{\gamma\kappa_0}{L_0}, \quad (15.78)$$

wherein $|y_{ss}| = y_0[E_i/E_\sigma]^{1/4}$ per Eq. (15.73), and $|\delta y_m|_{max}$ is the maximum value of the transient envelope reached along the bunch train. If $\eta < 1$ always, then the maximum is

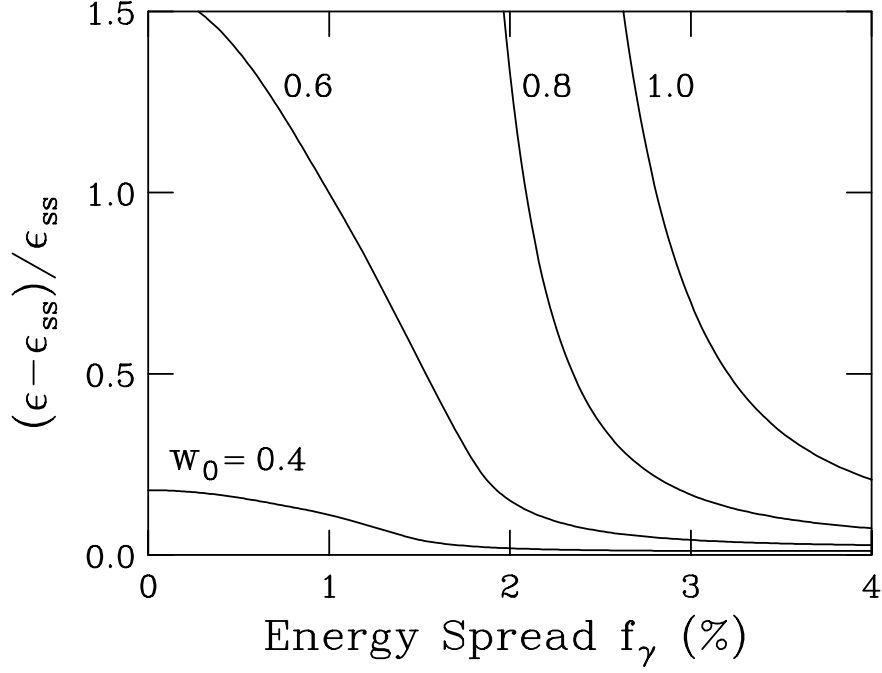


Figure 15.12: Total normalized transverse multi-bunch emittance at the linac exit, referenced to its steady-state value, versus total energy spread across the bunch train, plotted for various sum-wake amplitudes w_0 .

reached at the last bunch $m = M$. Otherwise, the maximum corresponds to the value of $|\delta y_m|$ at which $\eta = 1$. Imposing a focusing variation will reduce the transient envelope, but it also will establish a harmonic variation of y_{ss} with m and thereby introduce a nonzero steady-state emittance ε_{ss} . For this reason the quantity of interest is the ratio

$$(\varepsilon - \varepsilon_{ss})/\varepsilon_{ss} = \left(\frac{|\delta y_m|_{max}}{|y_{ss}|} \right)^2, \quad (15.79)$$

from which one sees the benefit of keeping the ratio of envelopes small. This quantity, calculated from the analytic expressions given in Eqs. (15.73) and (15.74), is plotted against $|f_\gamma|$ in Fig. 15.12 for various values of the sum-wake amplitude w_0 . Fig. 15.12 points to the region of parameter space that, respecting multi-bunch beam breakup, admits viable linear-collider designs. In particular it shows that to achieve low multi-bunch emittance without aid from a focusing variation requires small sum-wake amplitudes, $w_0 \lesssim 0.5$ V/pC/mm/m. Otherwise, as depicted, a few-percent energy spread relieves the constraint on sum-wake amplitude. There are, of course, practical limitations on the energy spread, to include longitudinal beam requirements at the interaction point,

lattice chromaticity, degradation in acceleration, etc. Nonetheless, introducing a modest energy spread constitutes a backup in case sufficiently low wake amplitudes prove generally infeasible.

It is worth mentioning that the plots in Figs. 15.10 and 15.12 have been performed with the data of the upgraded NLC. If we use the present lower energy design of accelerating the bunches up to only 500 GeV and 1.1×10^{10} particles per bunch, the reduction in adiabatic damping will increase the growths of the bunch deflections at the linac exit tremendously. To BNS damp such growths, an energy chirp of 10 to 15% will be necessary. Certainly this is not workable because of the large momentum spread of the bunches which later translates into unacceptable transverse bunch sizes at the interaction point. The acceleration gradient will also be largely reduced. Needless to say, the linac itself will hardly have such large energy aperture for the bunches to pass through. What we actually want to point out is that BNS damping is only feasible when the actual beam breakup is not too large, because only a small amount of energy chirp is acceptable in reality.

15.3.5.2 The Quality Factor

Now let us apply the computed displacement envelope to the DESY TESLA. If the quality factor of the deflecting wake were infinite, Eq. (15.77) would require an energy chirp of $|f_\gamma| = 9.27\%$. This chirp is rather large because of the long bunch train of 2820 bunches. Even with such a large chirp, Eq. (15.74) predicts a normalized transient displacement envelope of $|\Delta y_m/y_0| = 296$ for the last bunch at the linac exit, and such emittance growth is totally unacceptable. Fortunately, the transverse long-range wake of the TESLA linac in Fig. 15.13 shows considerable amount of damping [14]. However, the wake does not correspond to a damped resonance of a single frequency. Assuming a resonant frequency of 1.7 GHz, one obtains a quality factor of $Q = 22400$ by comparing the wake envelope at the first and 10th bunch spacings, $Q = 69000$ by comparing the wake envelope at the first and 100th bunch spacings, and $Q = 124000$ by comparing the wake envelope at the first and 265th bunch spacings (which is the end of the wake displayed in Fig. 15.13). In the discussion below, the quality factor of $Q = 125000$ is assumed. Numerically, we find that $|\Delta y_m/y_0|$ never exceeds 0.012 and damps to less than 0.010 within the first 150 bunches, where no energy chirp has been applied (see top plot Fig. 15.13 below). It is important to mention that the theoretical prediction of Eq. (15.74) may not apply to the TESLA linac, where MBBU is not severe because

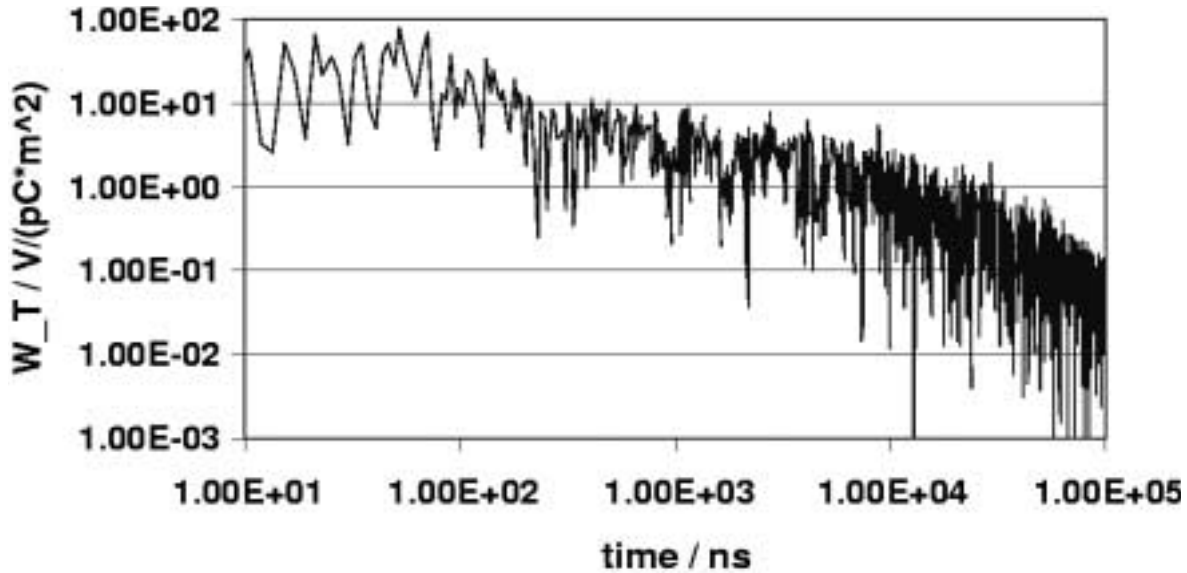


Figure 15.13: Plot of transverse long-range wake of the TESLA linac.

of the rather small effect from the transverse wake. Instead of the method of steepest descent, the MBBU equation should be solved by iteration with the coupling coefficient ϵ considered as a small quantity.

We can also visualize a finite quality factor Q of the deflecting wake as acting like an energy chirp. From the growth exponent of Eq. (15.74), it is evident that a finite quality factor will offset a certain amount of growth [13]. Setting $\eta = 1$ in the exponent, we obtain for the last bunch at the linac exit

$$|f_\gamma| = \frac{2M\omega_r\tau}{\pi^2 Q\nu_\beta}, \quad (15.80)$$

which is the equivalent amount of energy-chirp-like damping provided by the quality factor. In Fig. 15.14, we plot the normalized envelope displacement of the last bunch at the exit of the SLAC NLC linac as a function of the energy chirp $|f_\gamma|$ for various values of the quality factor. The large dots are the equivalent energy-chirp-like damping provided by the quality factor. The dashed curve joining all the large dots depicts Eq. (15.80). Notice that the displacement is approximately independent of the energy chirp until the stated threshold is exceeded, after which the displacement drops off relatively fast with increasing $|f_\gamma|$. As an illustration, recall that for a wake with an infinite quality factor, $|f_\gamma| = 2.18\%$ is required for BNS damping. However, when the quality factor is lowered to $Q = 5000$, Fig. 15.14 indicates an equivalent energy chirp of 0.96%. Thus,

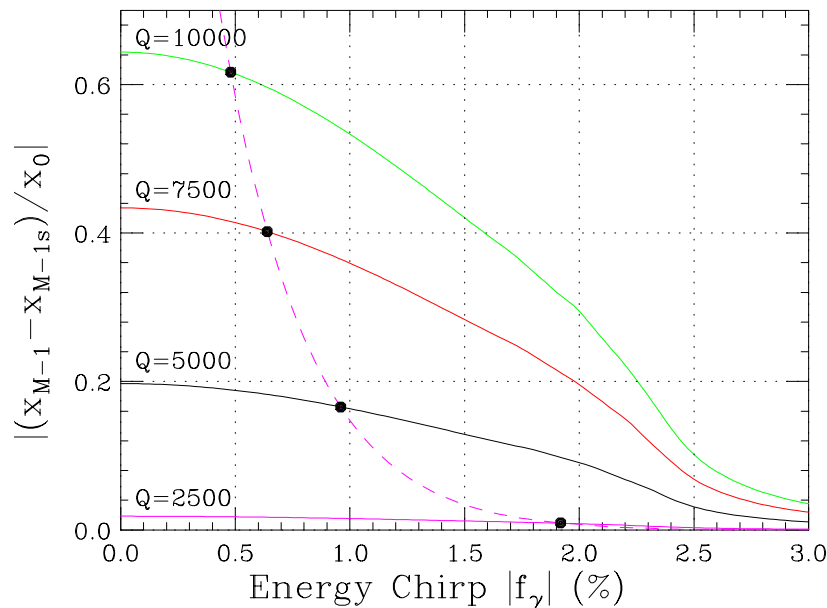


Figure 15.14: (color) Plot of normalized transient displacement envelope of the last bunch at the linac exit of the SLAC NLC versus energy chirp $|f_\gamma|$ for various quality factors Q of the deflecting wake. The amount of equivalent energy-chirp-like damping provided by the finite quality factor is also shown as dashes.

only $|f_\gamma| = 2.18 - 0.96 = 1.22\%$ will now be required. This is demonstrated in Fig. 15.15, where we can see the maxima of the displacement envelopes reside at the last bunch at the linac exit in both situations. A smaller quality factor not only reduces the amount of energy chirp required for BNS damping; it also helps to reduce the transient transverse displacement along the bunch train from $|\Delta y_m / y_0| = 0.76$ to a very much smaller value of 0.15. Thus, for the sake of controlling emittance growth and damping MBBU, it is beneficial to have lower quality factors for the deflecting modes. Returning to the TESLA linac, Eq. (15.80) gives an “effective” energy chirp of $|f_\gamma| = 4600\%$ for the last bunch of the bunch train and 1.6% for the second bunch ($M = 1$). This explains why the transient displacement envelope was so heavily damped.

15.4 Misaligned Linac

So far we have been considering linacs with perfect alignment, which is impossible in reality. Suppose that the quadrupole at location σ has misalignment $y_Q(\sigma)$ and the cavities have misalignment $y_A(\sigma)$ at location σ . The equation of motion governing the

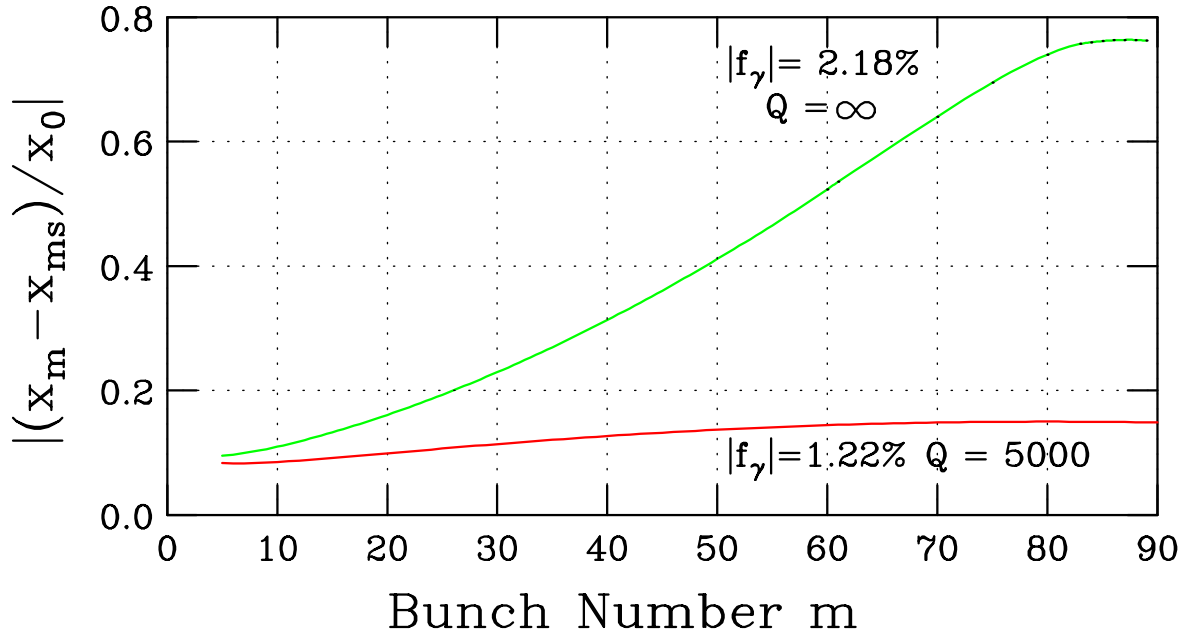


Figure 15.15: (color) Plot of normalized transient displacement envelope at the linac exit of the SLAC NLC when envelope maximum occurs at the last bunch. Notice that the energy chirp $|f_\gamma|$ is reduced from 2.18% to 1.22% when the quality factor is reduced from $Q = \infty$ to 5000.

transverse motion of the beam will be modified from Eq. (15.57) to [15]

$$\left[\frac{1}{\gamma} \frac{\partial}{\partial \sigma} \left(\gamma \frac{\partial}{\partial \sigma} \right) + \kappa^2(\sigma, \zeta) \right] [y(\sigma, \zeta) - y_Q(\sigma)] \\ = -\epsilon(\sigma) \int_0^\zeta d\zeta' w(\zeta - \zeta') F(\zeta') [y(\sigma, \zeta') - y_A(\sigma)] . \quad (15.81)$$

To arrive at an analytic solution, some assumptions are necessary. Consider the linac to be comprised of girders. On each girder is an accelerating length there are some number of rf structures and an optical element. Assume that the structures and quadrupoles are sufficiently well-aligned on the girders, leaving the girder misalignments as the dominant offset errors. If there are a large number of girders in each betatron wavelength, the beam will experience the same number of kicks due to the girder misalignments. Since the betatron wavelength is the characteristic *dynamic length*, the kicks act roughly as *white noise* on the beam. With these considerations, the quadrupole misalignment error $y_Q(\sigma)$ and structure misalignment error $y_A(\sigma)$ in Eq. (15.81) are the same random

variable. In other words,

$$\langle y_{Q,A}(\sigma_1)y_{Q,A}(\sigma_2) \rangle = \frac{d_g^2}{N_g} \Sigma(\sigma) \delta(\sigma_1 - \sigma_2) , \quad (15.82)$$

where N_g is the total number of girders in the linac and d_g is the rms girder misalignment. When the betatron focusing is strong, the MBBU equation can be solved in the same way as before when there were no misalignments. The result can be expressed analytically as

$$\frac{\langle \Delta y_m^e(\sigma)^2 \rangle^{\frac{1}{2}}}{\Delta y_m(\sigma)} \approx \frac{d_g}{y_0} \frac{2\pi\nu_\beta}{\sqrt{N_g}} \begin{cases} \frac{1}{\sqrt{\mathcal{E}(\sigma, m)}} & \eta \leq 1 \\ \sqrt{\frac{2}{3}} & \eta > 1 , \end{cases} \quad (15.83)$$

where $\Delta y_m^e(\sigma)$ is the transient displacement of the m th bunch in the bunch train which enters the misaligned linac without any displacement errors, while $\Delta y_m(\sigma)$, given by Eq. (15.74), is the transient displacement of the m th bunch in the bunch train which enters a perfectly aligned linac with initial displacement y_0 for all the bunches. The result is remarkable. First, it is simple. Second, it is independent of the amount of energy chirp f_γ either when $\eta \leq 1$ or $\eta > 1$. For $\eta = 0$, Eq. (15.83) reduces to Eq. (5.6) of Yokoya [16], which was derived without any energy chirp. The other difference from Yokoya is that his derivation is for the square roots of the total emittances rather than the transient displacements.

15.4.0.3 Comparison with Simulations

In order to reduce the fluctuations due to betatron oscillation, we try to compute the transient square-root-emittance $\Delta\epsilon_m^e$ instead of the transient displacement Δy_m^e , where the former is defined as**

$$\Delta\epsilon_m^e = \left[(y_m^e)^2 + (\beta y_m^{\prime e})^2 \right]^{\frac{1}{2}} - \left[(y_{ms})^2 + (\beta y_{ms}')^2 \right]^{\frac{1}{2}} , \quad (15.84)$$

with β being the betatron function at the location along the linac under consideration and $y_m^{\prime e}$ the divergence of the particle bunch. The subscript s denotes steady state. Thus, the left side of Eq. (15.83) is replaced by $|\langle \Delta\epsilon_m^e(\sigma)^{\frac{1}{2}} \rangle| / \Delta\epsilon_m(\sigma)^{\frac{1}{2}}$.

**The emittance defined here when divided by the betatron function is the usual unnormalized emittance.

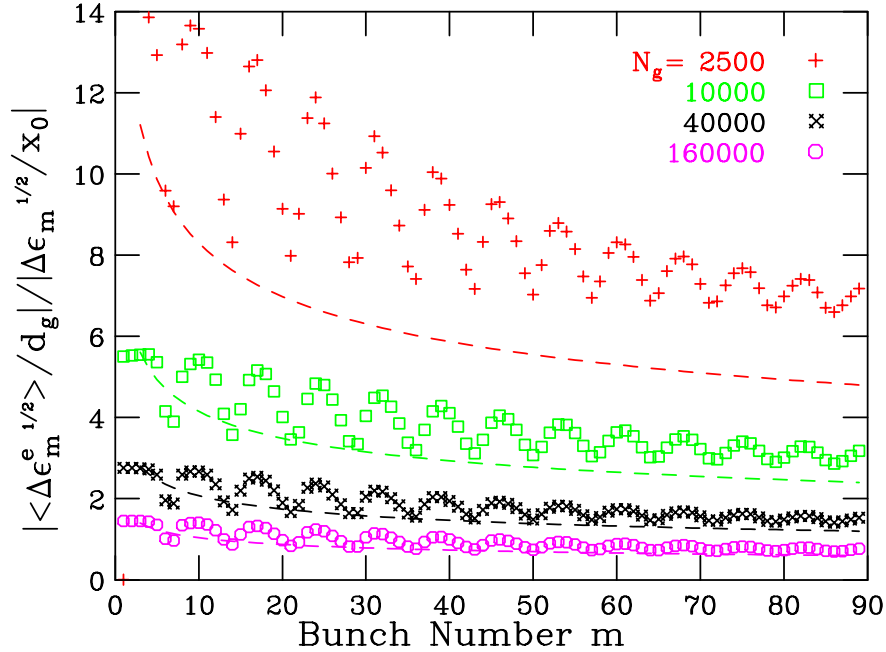


Figure 15.16: (color) Plot of ratio of transient square-root-emittance with girder misalignments but no beam offsets to that with beam offset but no girder misalignments at the linac exit of the SLAC NLC. The results verify the $N_g^{-1/2}$ dependency of the theoretical predictions which are shown here in dashes. The energy chirp is 1.0%.

We performed simulations of the SLAC NLC linac and computed beam quantities at its exit ($\sigma = 1$). In order to reduce the large spreads of the bunch displacements due to the randomness of the girder misalignments, each situation was simulated with 20 seeds and the results averaged. Figure 15.16 shows the simulated results when girder numbers $N_g = 2500, 10000, 40000,$ and 160000 were used, while the energy chirp was kept at $f_\gamma = 1.0\%$ all the time. The plot actually verifies the $N_g^{-1/2}$ dependency stated in Eq. (15.83). The theoretical predictions are also shown in dashes with the understanding that η is always less than unity. We see that Eq. (15.83) agrees with the simulated results, although it tends to underestimate the results in general^{††}. Actually, there will not be $N_g = 160000$ girders in the NLC linac. This number is created only for the purpose to check the theoretical prediction. With a linac length of $\ell = 10$ km and $\nu_\beta = 100$

^{††}The agreement of theoretical predictions with simulations would be as good as in Figs. 11 and 12 of Ref. [16] if we had plotted the simulation results of all seeds instead of just the averages and also with the vertical axis in a logarithmic scale.

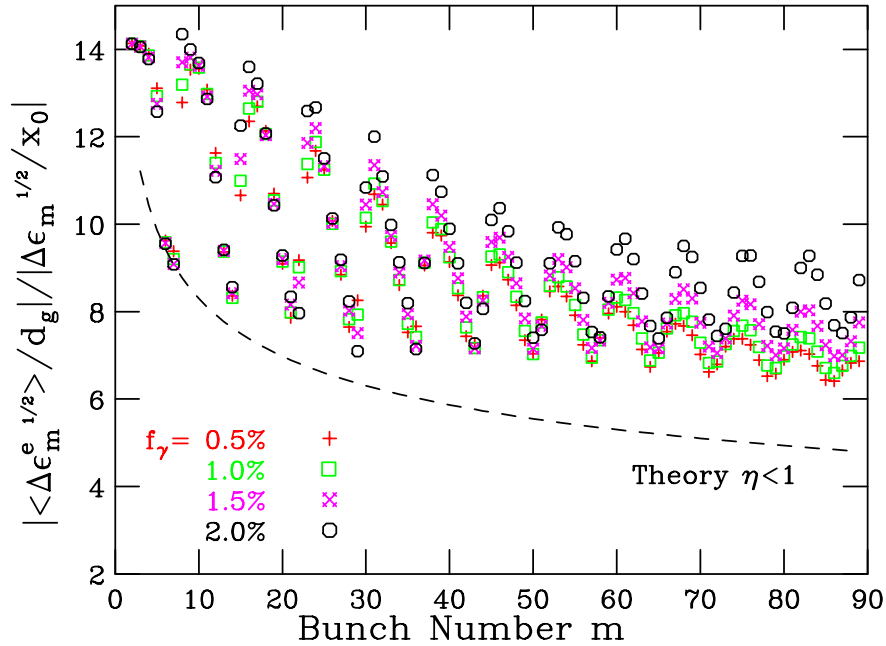


Figure 15.17: (color) Plot of ratio of transient square-root-emittance with girder misalignments but no beam offsets to that with beam offsets but no girder misalignments at the linac exit of the SLAC NLC with energy chirp $f_\gamma = 0.5, 1.0, 1.5,$ and 2.0% . The results appears to be f_γ -independent and follow the trend of the theoretical prediction for $\eta < 1$ shown here in dashes.

betatron wavelengths, $N_g = 2500$ may be a reasonable number, which will be used in the discussions below.

Next we vary the energy chirp to $f_\gamma = 0.5\%, 1.0\%, 1.5\%,$ and 2.0% . In all these cases, $\eta < 1$. We see in Fig. 15.17 that the simulation results fall on each other implying that there is no dependency on f_γ . Careful examination reveals that the ratio of the emittances appears to become larger for larger energy chirp especially when $f_\gamma = 2.0\%$. This is understandable, because the parameter η is closer to unity. The theoretical prediction is also shown; it appears to underestimate the simulation results.

Now let us examine the situation when $\eta > 1$. At the linac exit, η turns unity at the 48th bunch when the energy chirp $|f_\gamma| = 3.0\%$, at the 18th bunch when $|f_\gamma| = 5.0\%$, and at the 10th bunch when $|f_\gamma| = 7.0\%^\ddagger$. Simulations for these values of energy chirp

^{‡‡} $|f_\gamma| = 5$ and 7% would be unrealistically too high to survive the dispersive regions of the linear

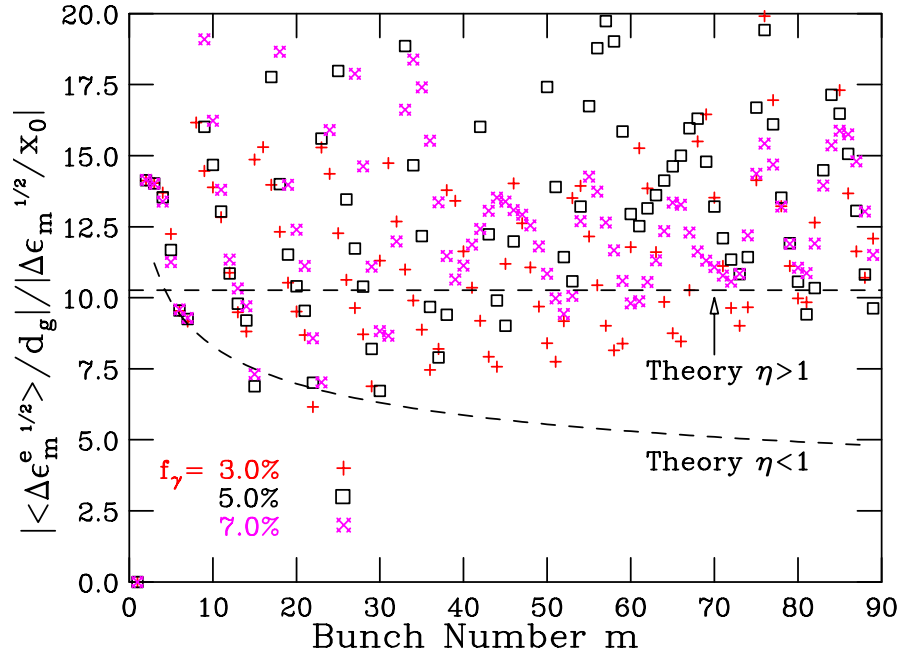


Figure 15.18: (color) Plot of ratio of transient emittance with girder misalignment errors but no initial displacement errors to that with initial displacement errors but no misalignment errors at the linac exit of the SLAC NLC with energy chirp $f_\gamma = 3.0, 5.0,$ and 7.0% . The results appear to be f_γ -independent and follow the trend of the theoretical prediction for $\eta > 1$ shown in dashes.

are shown in Fig. 15.18. First, these results appear to be f_γ -independent. Second, the ratios of emittances are definitely larger than those in Fig. 15.17 where $\eta < 1$. Third, these results are mostly bunch-number-independent, unlike those in Fig. 15.17. These observations lead us to conclude that the results follow the theoretical prediction for $\eta > 1$.

15.4.0.4 Application

We learn from Figs. 15.17 and 15.18 that the ratios of the normalized transient square-root-emittances are, respectively, of the order 5 ($\eta < 1$) and 10 ($\eta > 1$) for the SLAC NLC linac, implying that the emittance growth from girder misalignments is much more serious than the growth from beam misalignment at linac entrance. In Fig. 15.19, we

collider; $|f_\gamma| = 3\%$ is marginal.

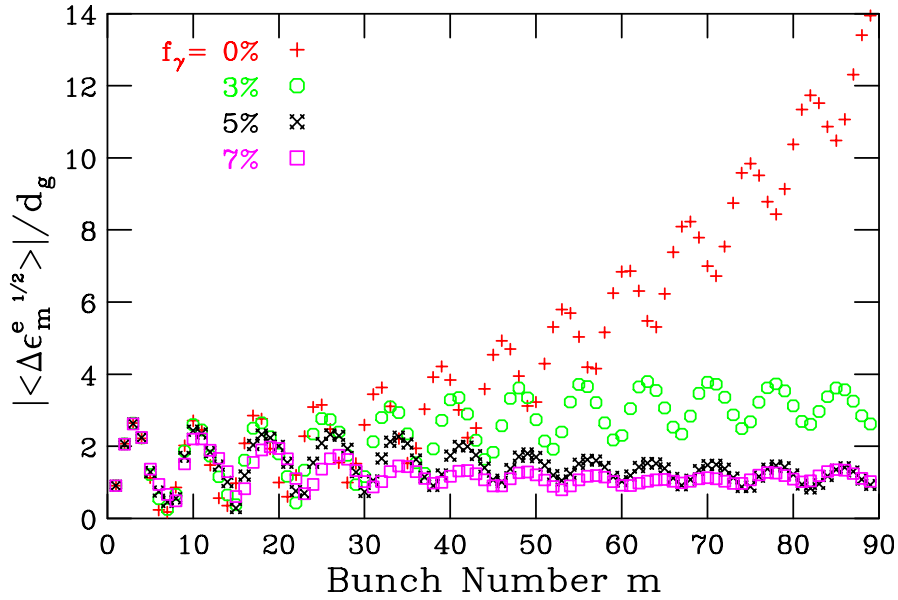


Figure 15.19: (color) Plot of transient square-root-emittance with girder misalignments but no beam offsets at the linac exit of the SLAC NLC with energy chirp $f_\gamma = 0.0, 3.0, 5.0,$ and 7.0% . Compared with Fig. 15.10, larger energy chirp will be necessary for BNS damping.

show the simulated normalized growth of transient square-root-emittance at the linac exit due to girder misalignment errors but without initial beam displacement errors. This growth is larger than the same growth of an initially displaced beam but without misalignment errors shown in Fig. 15.10. As a result, a larger energy chirp will be necessary to damp MBBU and control emittance growth. We see that although the growth saturates at an energy chirp of $f_\gamma < 3\%$, the normalized growth has been 4-fold, and one needs an energy chirp of 5 to 7% to lower the growth to within 2-fold. On the other hand, for an initially displaced beam in a perfectly aligned linac, a 3% energy chirp controls the growth to less than 0.5 as indicated by Fig. 15.10.

Let us come back to the TESLA linac. Because of the small influence of the transverse wake, the displacements of the bunches possess rather good memory of their initial offsets when injected into the linac. As a result, in the absence of an energy chirp, the transient displacements, $\Delta y_m(\sigma)$, for all the bunches are more or less in phase during their betatron oscillations along the linac. The envelope of $\Delta y_m(\sigma)$ will become rather sensitive to the location of observation. To avoid ambiguity, the transient square-root-emittance, $\Delta \epsilon_m^{1/2}$, defined in Eq. (15.84) must be used. The top plot of Fig. 15.20 shows

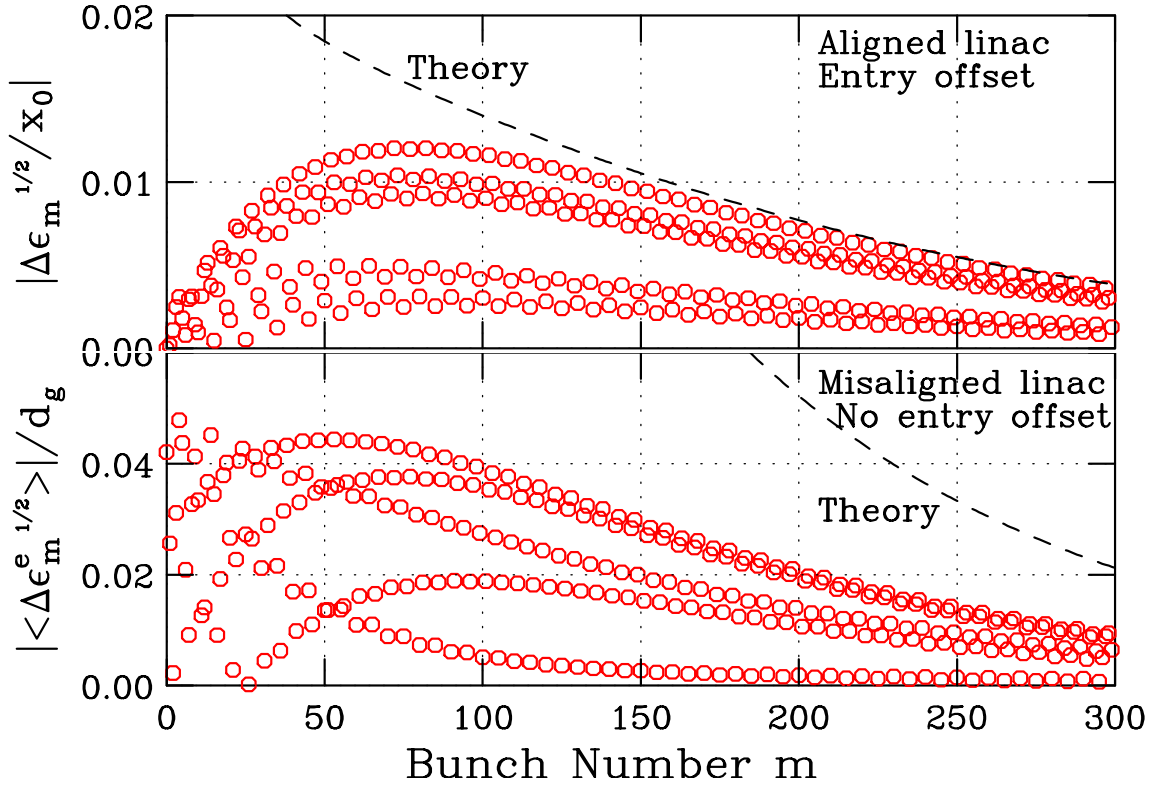


Figure 15.20: (color) Simulated normalized transient square-root-emittances for the first 300 TESLA bunches without energy chirp at the linac exit. Top plot is for bunches injected all with offset y_0 but no divergence in a perfectly aligned linac. Lower plot is for no injection offset, but the 2500 linac girders have rms misalignment d_g . Theoretical predictions are shown as dashes.

the simulated normalized transient square-root-emittance for a TESLA beam without energy chirp at the linac exit, where the linac elements are perfectly aligned while the beam is injected with the same offset y_0 but no divergence for all the bunches. We see that with an effective quality factor of $Q = 125000$, the maximum normalized transient square-root-emittance is small and completely acceptable, around ~ 0.012 near the beginning of the bunch train and rolling off to ~ 0.005 near the 300th bunch. The theoretical prediction [Eq. (15.74)] is shown as dashes, and unexpectedly agrees well with simulations for bunch number $m \gtrsim 150$. The lower plot shows the beam without offset at injection into the linac, but there are random misalignment errors in the 2500 girders. (Actually, each TESLA linac has less number of girders.) Although the normalized transient square-root-emittance becomes almost 4 times larger than the top plot, starting

with the maximum of ~ 0.045 and rolling off to ~ 0.012 near the 300th bunch, it is still acceptable. The theoretical prediction is shown as dashes and highly overestimates the simulation results. The disagreement is not hard to understand. Both Eqs. (15.83) and (15.81) do not apply well to the TESLA situation where the wake effect and MBBU are small. This prediction here is the product of the expressions in Eqs. (15.83) and (15.81) and therefore accumulates more uncertainty.

15.5 Exercises

15.1. (1) Assuming that the acceleration gradient is much less than the betatron wave number, derive the beam-breakup solutions, Eqs. (15.34) and Eq. (15.36), for the displacements of the head and tail in the two-particle model.

(2) The dipole transverse wake function of the SLAC linac per cavity cell at 1 mm is 62.9 V/pC/m. The bunch is of rms length 1 mm containing 5×10^{10} electrons. The cavity accelerating frequency is 2.856 GHz, with each cavity having the length of $\frac{1}{3}$ wavelength. The betatron wave number is $k_\beta = 0.06 \text{ m}^{-1}$. In a two-particle model, compute the ratio of the deflection of the tail particle versus that of the head particle along the whole linac. Compute the same ratio if the linac stays at 1 GeV without acceleration.

15.2. A linac has a lattice consisting of N FODO cells. In between two consecutive quadrupoles, there is an acceleration structure of length ℓ , which is half of the FODO cell length. The acceleration is linear with $E_f/E_i = 1 + 2N\alpha\ell$ where E_i and E_f are, respectively, the initial and final energy across the N FODO cells.

(1) Show that the transverse transfer matrix across the n th acceleration structure is

$$\begin{pmatrix} 1 & \frac{1+n\alpha\ell}{\alpha} \ln \frac{1+(n+1)\alpha\ell}{1+n\alpha\ell} \\ 0 & \frac{1+n\alpha\ell}{1+(n+1)\alpha\ell} \end{pmatrix}. \quad (15.85)$$

(2) Is the transfer matrix symplectic? Give a physical answer.

Hint: Solve Eq. (15.33) with $k_\beta = 0$.

15.3. The NLC bunch has an rms length of $\sigma_\ell = 150 \text{ }\mu\text{m}$ containing 1.1×10^{10} electrons. The linac has a length of 10 km, accelerating electrons from 10 GeV to 500 GeV. Assume a uniform betatron focusing with 100 betatron oscillations in the linac. The accelerating structure has a transverse mode at the mean frequency of $\bar{\nu} = 15.25 \text{ GHz}$ with an rms spread $\sigma_\nu = 25\%$ of $\bar{\nu}$.

(1) Use Eq. (15.44) to compute the transverse wake function at a distance σ_ℓ , assuming that the average kick factor is $\bar{K} = 40 \text{ MV/nC/m}^2$.

(2) Compute the multiplication factor of the tail particle in the two-particle model at the end of the linac.

(3) Assuming the natural chromaticity of $\xi = (\Delta k_\beta/k_\beta)/\delta = -1$ for the FODO-cell lattice, compute the energy spread between the head and tail of the bunch in

order to damp the deflection of the tail.

- 15.4. (1) Complete the derivation of the beam-breakup deflection of the m th bunch as given by Eq. (15.54).
- (2) For the NLC with 95 bunches with spacing 42 cm, estimate the deflection of the last bunch if the first bunch has an initial offset of $1 \mu\text{m}$. You may take the mean energy of the linac in the computation and the dipole wake at one bunch spacing as 0.21 MV/nC/m^2 .
- 15.5. Fill in the steps and give the estimate of the energy spread from the first to the 95th bunch in order to damp the beam breakup instability of the bunch train as outlined in Sec. 15.3.3.

Bibliography

- [1] C.M. Ankenbrandt *et al.* (Muon Collider Collaboration), Phys. Rev. ST Accel. Beams **2**, 081001 (1999).
- [2] E.-S. Kim, A.M. Sessler, and J.S. Wurtele, Part. Accel. Conf., March 29 - April 2, 1999, New York City, Article THP45.
- [3] V. Balakin, A. Novokhatsky, and V. Smirnov, Proc. 12th Int. Conf. High Energy Accel., Fermilab 1983, p.119.
- [4] V.E. Balakin, Proc. Workshop on Linear Colliders, SLAC, 1988, p.55.
- [5] K.L.F. Bane and R.L. Gluckstern, Particle Accelerators **42**, 123 (1993).
- [6] R. Jones, K. Ko, N.M. Kroll, R.H. Miller, and K.A. Thompson, *Equivalent Circuit Analysis of the SLAC Damped Detuned Structure*, EPAC'96, 1996, p.1292; R. Jones, K. Ko, N.M. Kroll, and R.H. Miller, *Spectral Function Calculation of Angle Wakes, Wake Moments, and Misalignment Wakes for the SLAC Damped Detuned Structures (DDS)*, PAC'97, 1997, p.551; R. Jones, N.M. Kroll, and R.H. Miller, R.D. Ruth, and J.W. Wang, *Advanced Damped Detuned Structure Development at SLAC*, PAC'97, 1997, p.548; M. Dehler, R.M. Jones, N.M. Kroll, and R.H. Miller, I. Wilson and J.W. Wuensch, *Design of a 30 GHz Damped Accelerating Structure*, PAC'97, 1997, p.518.
- [7] K. Yokoya, *Cumulative Beam Breakup in Large-Scale Linacs*, DESY 86-084, ISSN 0418-9833, 1986.
- [8] C.L. Bohn and J.R. Delayen, Phys. Rev. **A45**, 5964 (1992). "Multibunch Domain B" introduced in this reference is the limit of zero focusing variation away from wake zero-crossing.

-
- [9] C.L. Bohn and K.Y. Ng, Phys. Rev. Lett. **85**, 984 (2000); *Preserving High Multibunch Luminosity in Linear Colliders*, Fermilab Report FERMILAB-PUB-00-072-T, 2000.
- [10] G. Stupakov, talk given in SLAC-Fermilab Video Conference, September, 1999.
- [11] G. Stupakov, *Effect of Energy Spread in the Beam Train on Beam Breakup Instability*, SLAC Report, LLC-0027, 1999.
- [12] C.L. Bohn, Proceedings of the 1990 Linear Accelerator Conference, Los Alamos National Laboratory Report No. LA-12004-C, p. 306.
- [13] C.L. Bohn and K.Y. Ng, “Theory and Suppression of Multibunch Beam Breakup in Linear Colliders”, Proc. of XX Int. Linac Conf., Aug. 21-25, 2000, Monterey, CA.
- [14] TESLA Technical Design Report, DESY Report 2001-011.
- [15] K.Y. Ng and C.L. Bohn, *Theory of Cumulative Beam-Breakup with BNS Damping*, Proc. of 2nd Asian Particle Accelerator Conference, Sep. 17-21, 2001, Beijing, China.
- [16] K. Yokoya, “Cumulative Beam Breakup in Large-scale Linacs”, DESY Report 86-084, 1986.